

Merits and advances of microfluidics in the pharmaceutical field: design technologies and future prospects

Amr Maged^{a,b}, Reda Abdelbaset^c, Azza A. Mahmoud^{a*} and Nermeen A. Elkasabgy^d

^aDepartment of Pharmaceutics and Pharmaceutical Technology, Faculty of Pharmacy, Future University in Egypt, Cairo, Egypt;

^bPharmaceutical Factory, Faculty of Pharmacy, Future University in Egypt, Cairo, Egypt; ^cDepartment of Biomedical Engineering, Faculty of Engineering, Helwan University, Cairo, Egypt; ^dDepartment of Pharmaceutics and Industrial Pharmacy, Faculty of Pharmacy, Cairo University, Cairo, Egypt

ABSTRACT

Microfluidics is used to manipulate fluid flow in micro-channels to fabricate drug delivery vesicles in a uniform tunable size. Thanks to their designs, microfluidic technology provides an alternative and versatile platform over traditional formulation methods of nanoparticles. Understanding the factors that affect the formulation of nanoparticles can guide the proper selection of microfluidic design and the operating parameters aiming at producing nanoparticles with reproducible properties. This review introduces the microfluidic systems' continuous flow (single-phase) and segmented flow (multiphase) and their different mixing parameters and mechanisms. Furthermore, microfluidic approaches for efficient production of nanoparticles as surface modification, anti-fouling, and post-microfluidic treatment are summarized. The review sheds light on the used microfluidic systems and operation parameters applied to prepare and fine-tune nanoparticles like lipid, poly(lactic-co-glycolic acid) (PLGA)-based nanoparticles as well as cross-linked nanoparticles. The approaches for scale-up production using microfluidics for clinical or industrial use are also highlighted. Furthermore, the use of microfluidics in preparing novel micro/nanofluidic drug delivery systems is presented. In conclusion, the characteristic vital features of microfluidics offer the ability to develop precise and efficient drug delivery nanoparticles.

ARTICLE HISTORY

Received 28 February 2022

Revised 13 April 2022

Accepted 18 April 2022

KEYWORDS

Microfluidics; nanoparticles; micromixers; drug delivery; scale-up



1. Introduction

Microfluidics is the science that deals with the precise control of small volume fluid flow (directing, mixing, or separating) through networks of micro-scaled channels of different lengths and geometries. Compared to macro-scale flow, the dominating force in microfluidics is the viscous force, explaining the prevalence of laminar flow in the microchannels. In 1979, the birth of the first microfluidic device was introduced by Terry and his colleagues for gas chromatography (Terry et al., 1979). Then, Manz et al. and other researchers developed microfluidic platforms for electrophoresis and sample separation purposes at the beginning of the 1990s (Manz et al., 1990; Harrison et al., 1992; Mathies & Huang, 1992; Woolley & Mathies, 1994). Microfluidics was then used as a multidisciplinary breakthrough technology that was quickly established with wide applications as in environmental sensing (Vasudev et al., 2013; Pol et al., 2017), combinatorial chemistry (synthesis and assays) (Li et al., 2018; Liu et al., 2019), energy applications (Chen et al., 2018; De et al., 2020), micro-propulsion (Feng et al., 2015; Serrano et al., 2018), organ-on-a-chip technology (Sittadjody et al., 2021; Zheng et al., 2021), clinical diagnostics (Luo et al.,

2005; Chango et al., 2006), and drug delivery (Bains et al., 2017; Soheili et al., 2021). This review focuses on the application of microfluidics in drug delivery.

Microfluidics is applied for producing nano-ranged particles with tunable particle size (PS) and low polydispersity indices (PDIs). It is easy to use hazardous materials in microfluidics without exposure to carcinogenic samples. Microfluidic devices do not require large industrial spaces and ensure batch-to-batch reproducibility (Van Der Woerd et al., 2003; Zhang et al., 2020).

The production of nanoparticles using microfluidic devices is attributed to the high surface area to volume ratio of microchannels, resulting in uniform particle distribution, rapid transfer rates of heat and mass, and decreasing particle formulation time (Van Der Woerd et al., 2003; Zhang et al., 2020). All the previous pros distinguish microfluidic techniques over conventional production methods used to produce nanoparticles. Moreover, in the traditional techniques, the produced nanoparticles possess wide PS distribution, suffer from particles aggregations and loss, and separation using different preparation methods like nanoprecipitation, spray drying, and ultracentrifugation (Salafi et al., 2016; Maged et al., 2020; Adel et al., 2021; Niculescu et al., 2021).

CONTACT Nermeen A. Elkasabgy  nermeen.ahmed.elkasabgy@pharma.cu.edu.eg; nermeenadelahmed@outlook.com  Department of Pharmaceutics and Industrial Pharmacy, Faculty of Pharmacy, Cairo University, Kasr El-Aini Street, 11562 Cairo, Egypt

*Dr Azza A Mahmoud Azza.Ahmed@fue.edu.eg has contributed equally.

© 2022 The Author(s). Published by Informa UK Limited, trading as Taylor & Francis Group.

This is an Open Access article distributed under the terms of the Creative Commons Attribution-NonCommercial License (<http://creativecommons.org/licenses/by-nc/4.0/>), which permits unrestricted non-commercial use, distribution, and reproduction in any medium, provided the original work is properly cited.

One study conducted by Kang and his colleagues compared bulk mixing and parallel flow-focusing techniques during the preparation of polymeric nanoparticles. Results revealed the superiority of parallel flow-focusing in producing nanoparticles with monodisperse PSs (< 200 nm), while the bulk mixing methods failed to produce nanoparticles which might be attributed to the non-precise mixing of the process (Kang et al., 2013). In the same context, another study highlighted the success of microfluidics in the fabrication of magnetic chitosan nanoparticles loaded with cisplatin compared to the conventional co-precipitation method. The co-precipitation method produced broad particle-sized distributed nanoparticles with an average PS equal to 423 nm. On the other hand, the microfluidic method demonstrated nanoparticles with a narrow PS distribution, lower PS value equal to 104 nm, higher drug entrapment efficiency, and controlled drug release (Siavashy et al., 2021). The excellence of microfluidics over conventional bulk techniques is presented in another study led by Vu et al. The authors compared the fabrication of poly(lactic-co-glycolic acid) (PLGA) nanoparticles loaded with rutin using bulk emulsion evaporation process to those prepared using staggered herringbone micromixers. The nanoparticles prepared by microfluidics possessed smaller PS, uniform PS distribution, as well as higher drug entrapment, loading, and faster drug release than those prepared by bulk methods (Vu et al., 2019).

Despite the many benefits of using microfluidics in the production of nanoparticles, this method raises some limitations, such as cleaning the tiny microchannels, besides the possibility of clogging during sample streaming. Furthermore, the fabrication of microfluidic platforms is time-consuming and cost-intensive (Khan et al., 2015; Li et al., 2017; Martins et al., 2018; Seibt & Ryan, 2020).

Literature includes several examples presenting the use of microfluidics in the fabrication of different-sized particles. Among those examples are microparticles like micron-sized beads as alginate microgel (8–28 μm in diameter) (Ahmed & Stokke, 2021), PLGA magnetic beads ($\approx 60 \mu\text{m}$ in diameter), hybrid microgels (70–90 μm in diameter) (de Carvalho et al., 2021), and nanoparticles as gold nanoparticles (2–4 nm) (Al-Ahmady et al., 2019), citric acid-modified gold nanoparticles ($\approx 15 \text{ nm}$ in diameter) (Wang et al., 2019) and American ginseng polysaccharide nanoparticles ($\approx 20 \text{ nm}$ in diameter) (Akhter et al., 2019).

The main emphasis of this review is highlighting different microfluidic platforms and the factors affecting their operation. This review also discusses the techniques being applied to prepare different types of nanoparticles, the scale-up production approaches of nanoparticles, and innovative strategies for the practice of micro/nanofluidic drug delivery systems.

2. Principles of microfluidic mixers (micromixers)

Micromixing in microfluidics platforms has been applied in several fields like nanoparticles production, tissue engineering, and pathogen identification (Damiati et al., 2018; Hamblin & Karimi, 2020). The general structure of micromixer

includes many inlets, one outlet, and main mixing channel. Many researchers compete in the development of microfluidic designs to achieve high mixing efficiency. When developing microfluidic devices, several elements should be considered, including flow rates (FRs), inlets channels, and the shape of the main channel. Microfluidic parameters like FR as well as total flow rate (TFR) and flow rate ratio (FRR), which are the combined FRs of both phases (organic and aqueous) in the main mixing channel and the ratio between the flow of the two phases, correspondingly are considered the most important specific parameters (Zhigaltsev et al., 2012). Micromixers can be categorized based on the nature of fluid flow in the main mixing channel into two main catalogs, continuous flow (single-phase) and segmented flow (multiphase), as described briefly in Table 1 (Gonidec & Puigmartí-Luis 2018).

More details about the construction, types, and influencing factors on the microfluidic products of continuous and segmented flow micromixers will be discussed later.

2.1. Continuous flow (single-phase) microfluidic systems

Fabrication of nanoparticles in a continuous flow (single-phase) system involves the combination of fluids by diffusion in laminar flow streams that uses single or multiple solvents (Rhee et al., 2011; Clark et al., 2017). Diffusion is described as the process of molecules spreading from a higher concentration region to a lower concentration region through Brownian motion, resulting in gradual material mixing. Diffusion is explained mathematically using Fick's law (Fick, 1855):

$$j = -D \frac{d\varphi}{dx} \rightarrow \quad (1)$$

where j is the diffusive flux ($\text{mol}/\text{m}^2\text{s}^1$), D is the diffusion coefficient (m^2/s^1), φ is the species concentration (mol/m^3), and x is the position of the species (m).

The physical features of fluid flow in microfluidic channels are described by the Reynolds number (Re). The Re can be used to calculate the relation between inertial and viscous forces using the following formula (Reynolds, 1883):

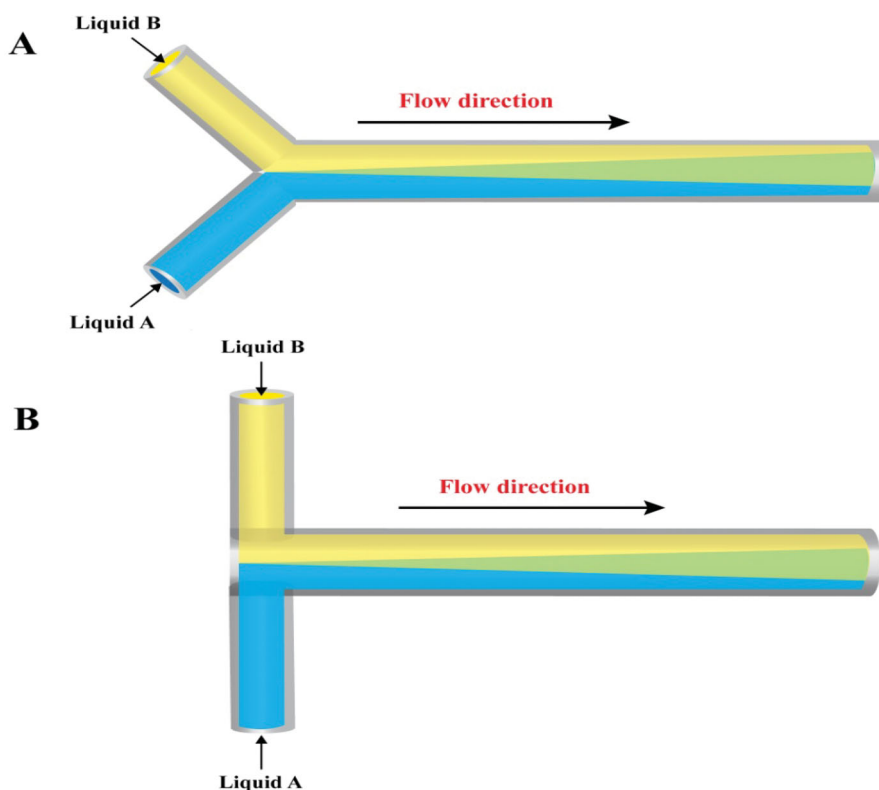
$$\text{Re} = \frac{\text{inertial force}}{\text{viscous force}} = \frac{\rho u L}{\nu} \rightarrow \quad (2)$$

where ρ is the fluid density (kg/m^3), u is the average flow velocity (m/s), L is the channel length (m), and ν represents the kinematic viscosity (m^2/s). Inside microfluidic system, flow is mainly laminar, with Re numbers often less than 100 (Wang et al., 2009). At low Re number values (<100), the viscous forces dominate the inertial forces, and a completely laminar flow occurs. Fluid streams flow parallel to each other in a laminar flow system, and velocity at every point within the stream is unchangeable with time (Beebe et al., 2002).

The simplest and most basic continuous flow microfluidic design is defined by either Y- (Therriault et al., 2003; Endaylalu & Tien, 2022) or T-shaped (Gobby et al., 2001; Ansari et al., 2018) channel micromixers (Figure 1(A,B)). However, the Re number is higher in T-shape than in Y-shape micromixers (Minakov et al., 2013).

Table 1. Comparison between continuous and segmented flow micromixers (Gonidec & Puigmartí-Luis 2018).

Types of the microfluidic platform	Principal	Features	Pros	Cons
Continuous flow (single phase)	The mixing is driven by the diffusion of reagents in laminar flow streams (turbulence-free condition) using a single or mixture of solvents	Reynolds number is less than one hundred (low)	A homogenous system that handled continuous flow streams	<ul style="list-style-type: none"> • Slow mixing • Fouling
Segmented flow (multi-phase)	Droplets are spontaneously generated using two immiscible phases as a result of both the external phase shear force on the inner phase as well as the interfacial tension of the two immiscible phases	The moving of slugs within a channel enhances solvents diffusion and chaotic mixing in liquid slugs	Fast mixing for nano- and femtoliter volumes	<ul style="list-style-type: none"> • In some cases, a high-efficiency downstream liquid separator is required to enhance the processing speed • Fouling in some cases

**Figure 1.** Y- and T-shaped micromixers: A) Y-shaped and B) T-shaped.

Mixing in these types of micromixers is entirely dependent on species diffusion at the liquid–liquid interface, which is sluggish and needs a lengthy mixing channel. Therefore, many techniques have been established to improve mixing efficiency in microfluidic devices. These techniques can be divided into passive and active mixing according to additional external energy input, whereas passive ones require no external energy input (Cai et al., 2017). Table 2 gives a brief overview on passive and active micromixers.

2.1.1. Passive micromixers

Mixing in passive micromixers is achieved using special geometries of microchannels, which are appealing since they are simple to be created besides do not have any external source of energy (Shanko et al., 2019). Various methods have been

proposed to improve their mixing efficiency like tuning the geometry of the main channel, FRs, and number of inlets.

2.1.1.1. Tuning the geometry of the main channel. Using more complex chaotic advection designs, the efficiency of Y- and T-shaped micromixers can be enhanced. Since it works to continually ‘stretch’ and ‘refold’ condensed solute volumes, chaotic advection improves mixing in laminar-flow systems, resulting in an exponential decrease in striation thickness. In microfluidic systems, chaotic advection can be accomplished by placing obstacles or changing channel geometries. Such change improves the flow stretching, folding, and splitting in each case. Zigzag channels, 3D serpentine channels, herringbone grooves, and spiral channels, are examples for chaotic advection-based micromixers (Shanko et al., 2019).

Table 2. Comparison between passive and active micromixers (Shanko et al., 2019).

Micromixer type	Passive	Active
Idea	Tortuous flow paths are used to mix the fluid streamlines, as well as the creation of chaotic advection.	Secondary flows are generated by applying an additional force, which speeds up the mixing phase.
Mixing	Y- and T-shaped, chaotic advection, parallel lamination, sequential lamination, flow focusing, coaxial, and toroidal micromixers	Pressure, sound (acoustic), electric, sound, magnetic, and thermal fields micromixers
Advantages	There is no need for external energy input.	Effective mixing while maintaining a low Re number.
Disadvantages	After primary production of the mixers, passive mixers are not controllable or adaptable, making them less resistant to improvements in real applications.	<ul style="list-style-type: none"> • Expensive. • It may be incompatible with biological components at sometimes.

In a zigzag micromixer, the laminar recirculation caused by zigzag angles (Re number < 80) can enhance the mixing efficiency as shown in [Figure 2\(A\)](#) (Lee et al., 2011). At high Re numbers, zigzag channels can produce chaotic advection through recirculating at the channel angles (Mengeaud et al., 2002).

A 3D serpentine microchannel can induce a chaotic flow of repeating segments in orthogonal planes, as shown in [Figure 2\(B\)](#) (Lee et al., 2011). A mixing segment is made up of two consecutive C-shaped parts which have planes that are perpendicular to one another. The flow field must be sufficiently 3D for mixing in the serpentine channel, with secondary flows stretching and folding the fluid, significantly raising the interfacial region in which diffusion occurs (Liu et al., 2000). The serpentine pipe, which is 3D, mixes significantly better than the straight channel (Liu et al., 2000).

Subjecting fluid volumes to a repeated series of rotational and extensional local flows is one way to create a turbulent flow. The staggered herringbone micromixer accomplishes this sequence of local flows by changing the shape of the grooves as a function of axial location in the channel, where the middle sites are swapped between half-cycles by changing the orientation of the herringbones. Ridges are located on the channel floor at an oblique angle of θ , with respect to the long axis (y), to produce transverse flows in microchannels using a steady axial pressure gradient ([Figure 2\(C\)](#)) (Carvalho et al., 2022).

As fluid goes downstream inside the spiral outlines, the amplitude of centrifugal forces increases, followed by an improvement in mixing performance. This is exploited in the design of spiral channel micromixers (Sudarsan & Ugaz, 2006). Transverse Dean flows are developed by simply adding curvature to the flow route due to centrifugal forces experienced by fluids going along a curved path, which offers increased mixing in a readily constructed flat 2D configuration ([Figure 2\(D\)](#)) (Erdem et al., 2020).

Sequential lamination micromixers depend on dividing the incoming stream into two channels and then reunite them; this process can be done multiple times to enhance the contact area between the laminae. Sequential laminations are also known as Split and Recombine (SAR) micromixers ([Figure 2\(E\)](#)). Mixing in SAR micromixers is enhanced at low Re numbers, therefore, they are good for viscous fluids. The disadvantage of this kind of micromixers is that it requires a three-dimensional manufacturing procedure,

which makes it more difficult to manufacture (Kang et al., 2013; Siavashy et al., 2021).

2.1.1.2. Tuning the flow rates. Flow focusing micromixers consist of three inlets and one outlet. The fluid stream to be mixed flows down the middle channel, meeting two nearby streams running at greater FRs in hydrodynamic flow focusing ([Figure 3\(A\)](#)). The middle stream is squeezed into a small channel between the two neighboring streams when Re numbers are low. Reducing the stream width (middle stream) allows quick mixing through diffusion (Knight et al., 1998).

Similar, the conical design of the micropipette makes it simple to focus the inner capillary liquid flow inside the outer capillary ([Figure 3\(B\)](#)). A laminar flow regime characterizes the coaxial flow. A micromixer with a coaxial flow achieves short diffusion distances and fast mixing times (Abou-Hassan et al., 2009).

2.1.1.3. Tuning the number of inlets. The parallel lamination mixer consists of numerous coaxial channels that coalesce into a single narrow channel. This kind of micromixers improves the mixing operation by reducing the diffusion duration and increasing the contact surface area between the two fluids ([Figure 3\(C\)](#)) (Ehrfeld et al., 1999; Erbacher et al., 1999; Löb et al., 2004).

2.1.2. Active micromixers

As clarified in [Table 2](#), several techniques for active mixing are conducted. However, this review will discuss two of the most used active mixing techniques for the fabrication of drug delivery particles, namely, pressure field disturbance, and acoustic micromixers.

In a pressure field disturbance micromixer, the performance of basic micromixer (Y- or T- shaped) can be enhanced when both inlets of any of the micromixers are pulsed at the same time. Consequently, the boundary between the two liquids is extended over the mixing zone, which improves mixing ([Figure 4\(A\)](#)) (Shanko et al., 2019). Furthermore, the mixing within the micromixer can be enhanced if both inlets are pulsed with a 180° phase difference. Pressure field disturbance improves mixing between two reagents by regularly changing FR in the two inlet channels without additional geometric features, components, or external fields (e.g. electric, magnetic, etc...) (Glasgow & Aubry, 2003). The pressure difference can be generated either using an

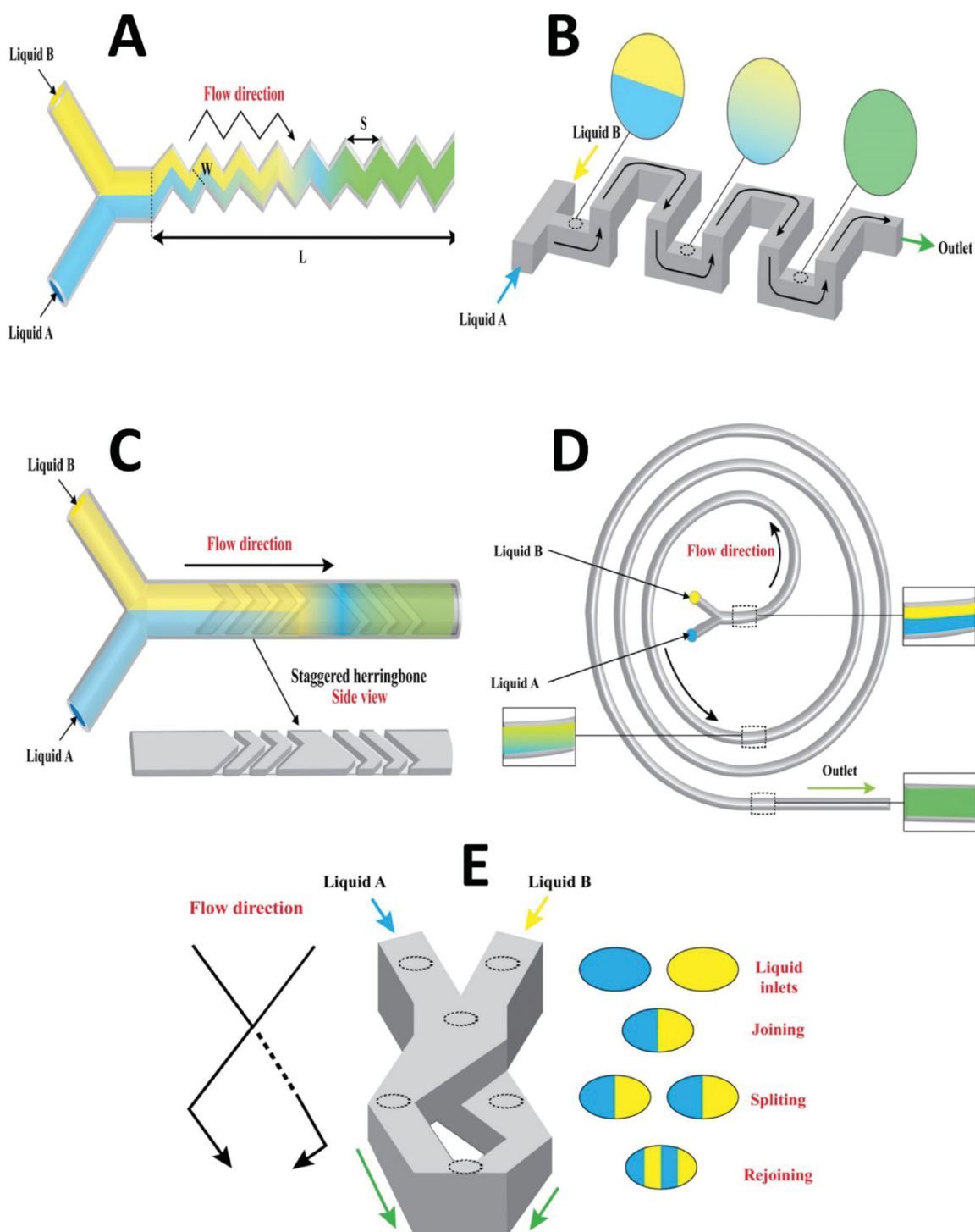


Figure 2. Chaotic advection passive micromixers; A) Zigzag channel, B) 3D serpentine channel, C) Herringbone grooves channel, D) Spiral channel micromixers, and E) Sequential lamination channel (Split and Recombine channels) (Redrawn under permission of Elsevier from reference (Hamdallah et al., 2020)). W is the channel width, S , and L are the linear length of the periodic step and the zigzag microchannel, respectively.

external micropump (Fujii et al., 2003) or an inbuilt planar micropump (Deshmukh et al., 2001).

Acoustic actuators are used in micromixers to stir fluids in a transverse direction to the flow direction, resulting in better mixing inside the microfluidic channel (Figure 4(B)) (Yang et al., 2000; Yaralioglu et al., 2004; Shanko et al., 2019). The acoustic waves can be generated by integrated piezoelectric ceramic transducers (Yang et al., 2001; Shanko et al., 2019). Since many biological fluids are temperature sensitive, the

major disadvantage of an acoustic-based micromixer is the generated temperature.

2.2. Segmented flow (multiphase) microfluidic systems

Droplets are created in segmented flow microfluidic systems by mixing two immiscible phases (dispersed phase and continuous phase). Droplet generation is a natural phenomenon

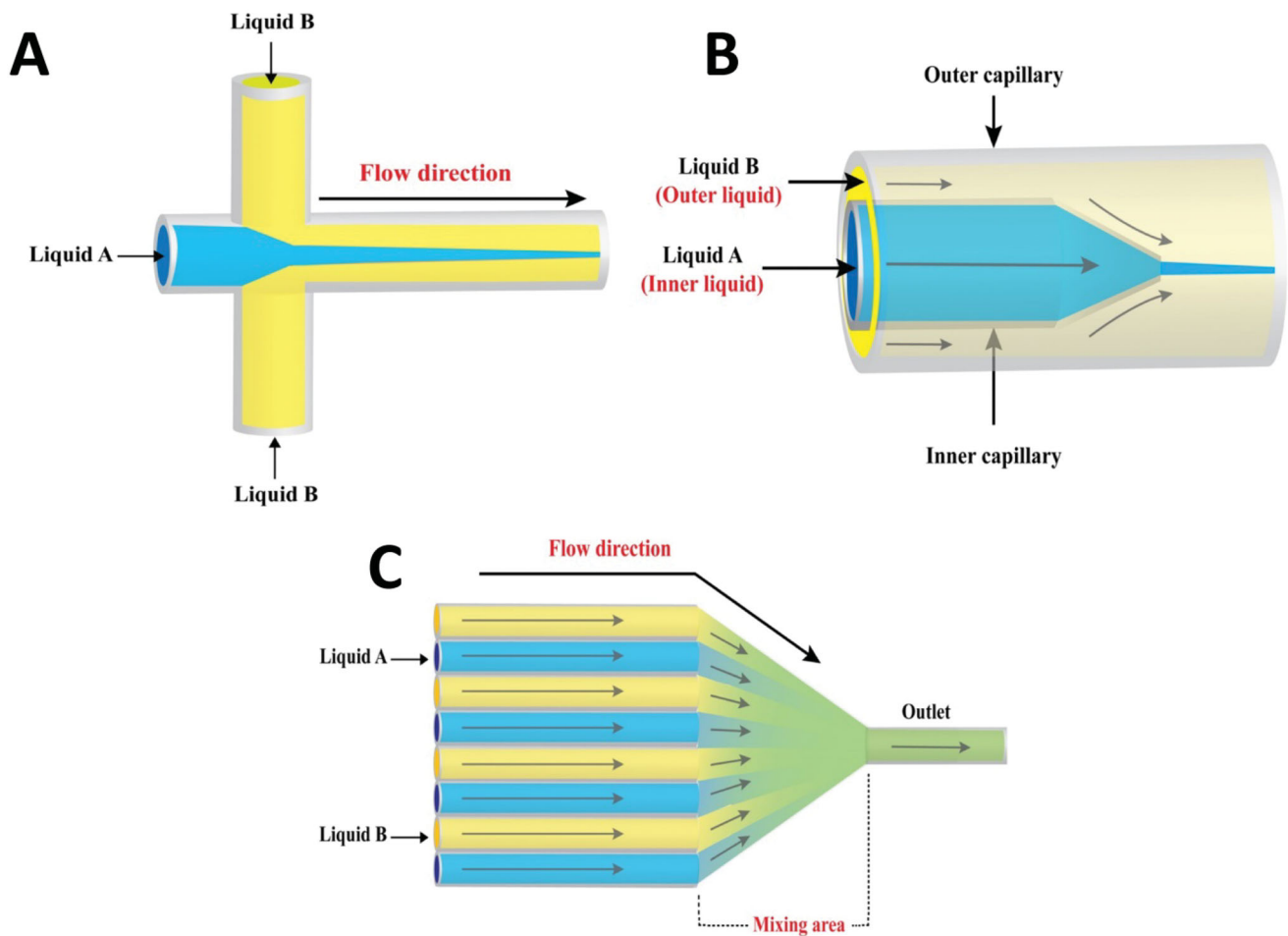


Figure 3. A collective diagram representing different passive micromixers; A) Flow focusing channel (Redrawn under permission of Elsevier from reference (Lu et al., 2016)), B) Coaxial channel micromixers (Redrawn under permission of Elsevier from reference (Vladislavjević et al., 2013)), and C) Parallel lamination channel (Redrawn under permission of Elsevier from reference (Sabry et al., 2018)).

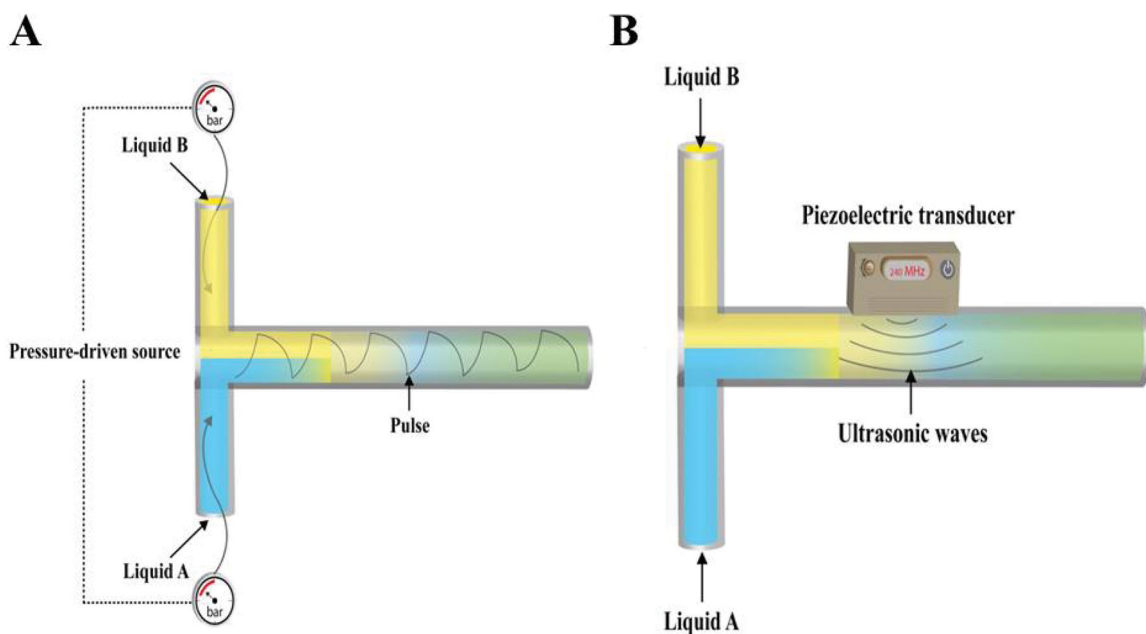


Figure 4. Active micromixers; A) Pressure field disturbance and B) Acoustic micromixers.

that is usually triggered by shear force and interfacial tension at the fluid–fluid interface (Thorsen et al., 2001; Tice et al., 2003; Günther & Jensen, 2006; Shui et al., 2007a).

Capillary number (Ca) is a parameter that describes multi-phase flow activity in microchannels by expressing the competition between viscous and interfacial forces as defined in

the following equation (Yang et al., 2001):

$$Ca = \frac{\mu u}{\gamma} \rightarrow \quad (3)$$

where μ (m^2/s) is the continuous phase viscosity, u (m/s) is the average flow velocity, and γ (N/m) is the interfacial tension between both fluid phases.

Droplet sizes may be controlled by varying the cross-sectional dimensions of microchannels, and reagents concentrations can be controlled by varying the FR (Bringer et al., 2004). As each droplet is separated from others, hence it operates as an independent reaction vessel. In straight channels, a recirculation motion is induced by the addition of a new phase, causing stretching, and folding of a solution, which improves mixing efficiency in the same way as chaotic advection (Figure 5(A)). The recirculation inside the segmented flow can be controlled by fluid velocities. At low velocities, the interfacial tension is insufficient to induce full recirculation, but at high velocities, quicker convection within full recirculation leads to higher mixing performance (He et al., 2020). When the flow is deformed along a curved channel, the axisymmetric circulation flowing in each compartment breaks and the substances disperse making the twisting channel a significant route for better mixing (Figure 5(B)) (Song & Ismagilov, 2003; Demello, 2006).

T-junction and flow focusing are the commonly utilized channel geometries to create droplets in microfluidic channels (Anna et al., 2003; Shui et al., 2007b; Shembekar et al., 2016; Deng et al., 2019). In T-junction microchannel devices, the dispersed phase is provided by a microchannel perpendicular to a main channel in which the continuous phase flows (Figure 6(A)). At the intersection of the two microchannels, or further downstream, the thread breaks apart and droplets form. It is indeed possible to adjust the dimensions of the formed microdroplets by adjusting the viscosity of the two phases, FR or channel dimension (Jamalabadi et al., 2017).

In flow focusing channels, the dispersed phase is supplied through the central channel, while the continuous phase is delivered in opposing directions from two lateral channels (Figure 6(B)) (Basova & Foret, 2015; Chou et al., 2015). Due to the streaming of the continuous phase into the two lateral channels; strain and shear forces are built onto the inner fluid, forming a narrow neck that progressively collapses, leading to the creation of a droplet. The viscosity of the two phases and their FR are critical in controlling droplet generation in this design (Capretto et al., 2011).

Besides the classification based on geometric configuration, segmented flow microfluidic systems can also be categorized depending on the nature of the mixed phases into both gas-liquid flow and liquid-liquid flow systems (Figure 6) (Chou et al., 2015).

Surfactants are often used in a liquid-liquid flow, such as water-in-oil and oil-in-water dispersions, to prevent the scattered droplets from coalescing (Baret, 2012). The FR and chip geometry have a strong influence on the droplet morphology. Nanoparticles of various sizes and shapes are synthesized in liquid-liquid flow systems due to adequate mixing effectiveness and mass transfer (Duraiswamy & Khan, 2009;

Niu et al., 2015). Nanoparticles can be fabricated with greater reproducibility because the reacting solutions are encapsulated within liquid droplets, which greatly reduce pollution and channel clogging. Figure 6(A,B) represents the liquid-liquid flow microfluidic systems (Chou et al., 2015).

In gas-liquid systems (Figure 6(C)) (Chou et al., 2015), it is often seen as a bubbly flow that disperses in a liquid phase (Gunther et al., 2005; Yu et al., 2007). By developing recirculation, incorporating the gas phase will significantly increase mixing efficiency (Zhao et al., 2011). The quick isolation of the gas from the produced dispersion to get the desired nanoparticles is one of the most appealing features of gas-liquid segmented flow reactors (Gunther et al., 2004; Khan & Jensen, 2007). However, it has the potential for clogging, which can be evaded with liquid-liquid flow reactors (Yen et al., 2005; Krishna et al., 2013).

3. Approaches for efficient microfluidics

There are numerous obstacles to using microfluidics in the pharmaceutical field, including the materials used for the construction of the microchannels, their design, associated equipment like pumps, and the used materials for the fabrication of nanosystems. The complex interplay between those factors can further influence the fabrication process. Going through the path of success for the whole process requires a complete understanding of all these challenges and finding suitable approaches to solve them. This section sheds light on some approaches applied to enhance the efficacy of microfluidics. Among those approaches are those related to the construction of microchannels, like surface modification of the constructive materials, besides avoiding the adsorption of foulants on the internal surfaces of microchannels. Another approach is related to the purification and concentration of the produced nanoparticles, known as post-treatment.

3.1. Surface modification

Microfluidic fabrication methods are classified according to the microfluidic fabrication material, silicon/glass, or polymer. Glass/silicon-based microfluidic devices are fabricated using lithography and etching techniques (Kim et al., 2019; Vasilescu et al., 2020). Polymer-based microfluidics are fabricated using lithography (Mukherjee et al., 2019; Kajtez et al., 2020), laser ablation (Shaegh et al., 2018; Gao et al., 2019; Hu et al., 2020), injection molding (Li et al., 2020; Ma et al., 2020), hot embossing (Lin et al., 2017; Lauri et al., 2019) and 3D printing (Macdonald et al., 2017; Romanov et al., 2018; Vasilescu et al., 2020).

Surface wettability plays an essential role in microfluidics, especially in controlling liquid flow and the motion of the droplets. The solid surface can interact with the liquid through the intermolecular forces between their molecules. Wettability affects the spreadability of liquid in microfluidics, and the ability of the liquid to spread can be measured using the contact angle between the solid surface and liquid (θ), the decrease in surface wettability (high contact angle-

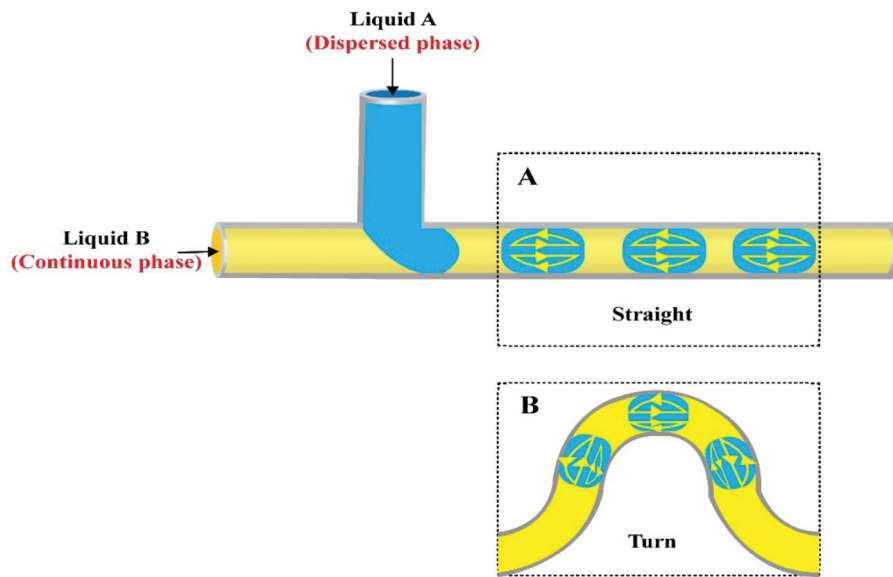


Figure 5. Mixing within slugs (Redrawn under permission of Elsevier from reference (Sivasamy et al., 2010); A) Straight and B) Serpentine-shaped channels.

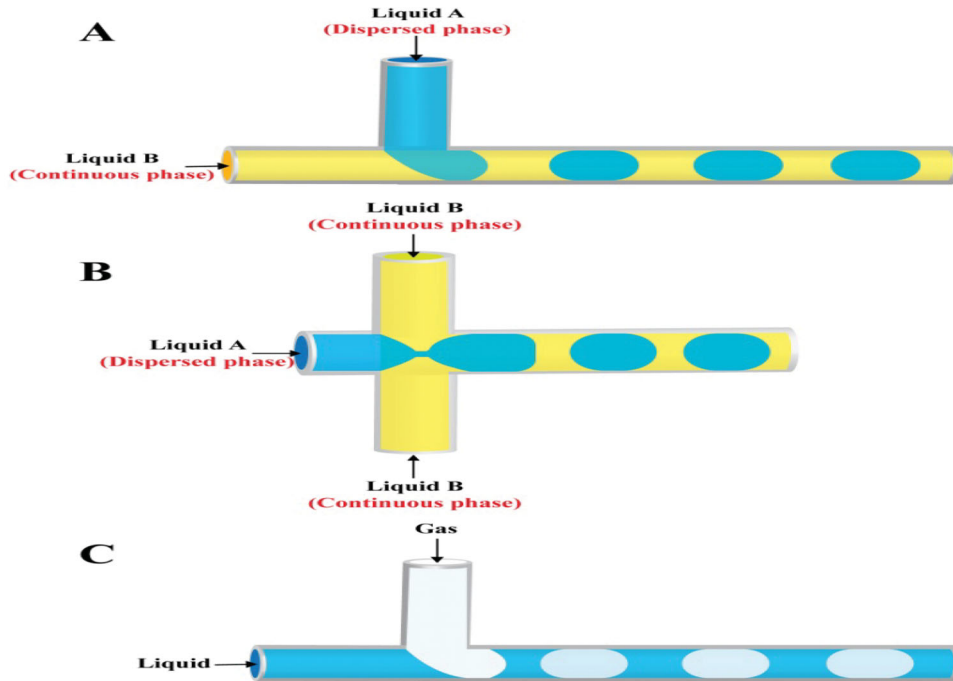


Figure 6. Segmented micromixers: A) T-configuration, B) Flow focusing, and C) Gas-liquid multiphase.

value) means decreasing the spreading behavior of the liquid. Generally, the contact angle values less than or equal to 90° show the spreadability of liquid, while the highest values of spreadability and wettability can be achieved with contact angle values near 0° (Saxena & Joshi, 2020).

Contact angle manipulation is relevant in enhancing mixing efficiency besides preserving the integrity of microchannels when using microfluidic platforms. Most of the materials used in microfluidics fabrication are hydrophobic with low surface energy and low adherence properties to other materials. This hydrophobicity leads to increased pressure and resistance of a liquid to flow through the microchannels. The most popularly used polymers in the fabrication of microfluidics include polymethyl methacrylate (Matellan & Armando,

2018; Kotz et al., 2020), polyvinyl chloride (Sitanurak et al., 2019; Samae et al., 2020), and polyethylene terephthalate (Cui et al., 2020; Kim et al., 2021), and polydimethylsiloxane (PDMS) (Hiltunen et al., 2018; Akther et al., 2020; Ferraz et al., 2020).

PDMS is considered a hydrophobic material with a contact angle of more than 100° . Therefore, the unmodified PDMS is restricted to producing water in oil emulsion (w/o) (Mata et al., 2005). In order to increase the hydrophilic properties of PDMS, surface modifications can be done using ultraviolet irradiation, oxygen plasma (Long et al., 2017; Ruben et al., 2017; Zhu et al., 2020), corona discharge (Bashir et al., 2018), layer by layer deposition (Choi et al., 2018; Zhang et al., 2019), sol-gel methods (Abate et al., 2008), and surface

treatment with surfactant (Fu et al., 2017; Khemthongcharoen et al., 2021). Using oxygen plasma, PDMS-based microfluidic surface modification carried out by Long et al. showed a contact angle of less than 10° . Unfortunately, the hydrophilicity of PDMS disappeared after two hours of practical use. The addition of polyethylene glycol (PEG) coating with oxygen plasma resulted in persisting surface hydrophilicity within 420 h after practical use with contact angles values ranging between 3.5° and 67.7° (Long et al., 2017). Jahangiri and his team succeeded in maintaining the surface hydrophilicity of PDMS treated with oxygen plasma for 100 d. The study was performed in different storage conditions; at room temperature, -15 and -80°C . The study proved the preservation of microchannels properties and contact angles in the colder temperature without changing the geometrical obstacles of microchannels for longer times (Jahangiri et al., 2020).

Although decreasing the contact angle of PDMS (increasing hydrophilicity) showed superiority in the aforementioned examples; however, this was not the case when organic solvents were streamed through the microchannels due to the swelling of PDMS as well as solvent adhesion to the wall of microchannels. A solution for this case was introduced by Mahmoodi and his colleagues who coated the PDMS surfaces with polytetrafluoroethylene (PTFE) nanoparticles to easily stream dexamethasone-loaded PLGA nanoparticles (prepared using dichloromethane (DCM) as an organic solvent) without any adhesion to the wall of microchannels due to low surface energy and low adhesive properties of fluoropolymer coating. The coating was carried out by injecting a solution of PTFE nanoparticles (60% w/v) through microchannels using a syringe pump. The PTFE film was deposited and formed after subjecting the microchannels to elevating temperatures of 70 and 150°C for 10 and 25 min, respectively, in the oven. The coating layer of PTFE revealed a surface with high hydrophobic properties. The contact angle reached 140.3° , preventing dexamethasone nanoparticles aggregation and adhesion during streaming in an organic solvent and preventing swelling of the wall of microchannels. This surface-modified microfluidics succeeds in preparing dexamethasone nanoparticles with PS values ranging between 47 and 82 nm with high encapsulation efficiency values of more than 80% (Mahmoodi et al., 2019).

In addition to the swelling ability of PDMS-based microfluidics using an organic solvent, PDMS does not show resistance to the heating process required to fabricate solid lipid nanoparticles. To overcome this problem, Arduino and his team successfully fabricated solid lipid nanoparticles at a temperature of 60°C using microfluidic devices made of borosilicate glass capillaries and glass rods (Arduino et al., 2021). The glass-based microfluidic devices were resistant to organic solvent and heat and did not disrupt microchannels' features (Liu et al., 2015; Arduino et al., 2021).

3.2. Anti-fouling

Why do dispersed particles or droplets, flowing in microchannels, deposit onto the walls? An important question

highlights a significant limitation known as 'fouling in microfluidic channels' (Cejas et al., 2018). Fouling is the irreversible adsorption of foulants onto the microchannels (Jung et al., 2019). Suppression of fouling is highly required for better investigation of optimum concentrations, FR, and other factors needed for the production of reproducible, tunable nanoparticles. The underlying cause for fouling may be due to the laminar flow in straight microchannels, which is not enough for achieving rapid, efficient convective mixing (Dietzel, 2016). A proposed solution for this problem is represented in speeding up the mixing of fluids inside the channels, either by designing different geometric configurations like flow-focusing or using built-in mixers inside the channels (Lorenz et al., 2018; Stolzenburg et al., 2018). A free jet (Marmioli et al., 2009) and staggered herringbone micromixers (Jung et al., 2019) overcame the fouling onto the walls.

However, it was previously stated that even in segmented flow micromixers, the fouling effect might occur depending on the type of lipid used (Riewe et al., 2020) besides the surface properties of the inner channels (Erflle et al., 2019); shedding light on the proper selection of components and experimental setup, as well. The solubility of the lipid is of great importance; Softisan[®] 100 (a blend of solid triglycerides) ethanolic solution resulted in fouling in a segmented flow micromixer due to its low solubility in ethanol, resulting in its crystallization (Erflle et al., 2017). However, using more ethanol soluble lipids, i.e. castor oil and glyceryl monooleate, avoided the fouling effect. Additionally, the use of Tween[®] 80 (with good aqueous and ethanolic solubility) offered fast stability for the oil droplets evading the fouling effect (Riewe et al., 2020).

During the process of preparing lipid-based nanoparticles (castor oil nanoemulsion and glycerol monooleate nanoparticles) using a segmented gas-liquid flow micromixer, a fouling problem appeared through the deposition of oil droplets onto the channel's walls (Riewe et al., 2020). This issue led to the formation of large oil droplets that may gradually be washed away, leading to contamination of the collected particles. Such a problem was reduced in the nanoemulsion preparation when Tween[®] 80 was added to the ethanolic solution instead of the aqueous solution, which efficiently stabilized the interfacial surface of castor oil. In the same context, as glycerol monooleate can form liquid crystals, this problem resulted in fouling while preparing lipid-based nanoparticles due to the formation of thin film of liquid crystalline cubic phase. Fouling effect was reduced by decreasing the ethanol channel diameter from 58 to $29\ \mu\text{m}$, which might be endorsed to: (1) reduced backflow of aqueous stream to the ethanol channel during the formation of gas bubble and thus decreased oil deposition at the junction between the two channels and (2) reduced backflow of ethanol to the water channel that could lead to lipid supersaturation on the wall of the channel. However, both used diameter values did not cause any significant change in PS values and PDI for both types of lipid-based nanoparticles.

Other studies highlighted the effect of surface smoothening on reducing the fouling effect permitting for a sustained,

stable process (Erflé et al., 2019). A published study compared the effect of the surface roughness of inner microchannels on the intensity of fouling. Laser ablation, etching, and tempering of microchannels were attempted. Results revealed that the surface roughness was maximum after laser ablation (0.41 μm) but minimum after the tempering process (0.09 μm), which was attributed to the use of high temperatures during tempering (760 °C for 1 h), resulting in melting of glass, formation of highly viscous liquid which covered any round pits and cavities hence higher smoothness of channels surfaces was obtained. Getting rid of any pits and cavities on the surfaces will avoid the deposition of particles or droplets, which can act later on as nucleation points for further fouling (Erflé et al., 2019).

Modifying the inner surfaces of the microchannels was addressed in another study, preparing gold nanoparticles to suppress fouling phenomena. Silanization of the inner surfaces with trichloro(1H,1H,2H,2H-perfluoro-octyl) silane led to increased hydrophobicity thereafter less wetting and fouling. This study also highlighted the effect of pH control on the degree of fouling. Results revealed that at high pH values, fouling was much reduced, which was endorsed by the repulsion created between the formed nanoparticles (negative charged) and the inner surfaces (Wagner & Köhler, 2005), emphasizing the importance of electrostatic repulsion in alleviating the fouling problem.

Generally, fouling cannot be abolished entirely; however, it should be minimized to extend the shelf life of microchannels.

3.3. Post-microfluidic treatment

The preparation of nanoparticles using microfluidic devices depends mainly on nanoprecipitation techniques. The polymers, lipids, or drugs are dissolved in organic solvents which are then mixed with an aqueous phase inside the microchannels, forming the nanoparticles.

Using organic solvents, if they remained in contact with the formed nanoparticles, could affect their stability resulting in infused particles due to Ostwald ripening, enhancing the possibility of drug leakage (Kumar & Prud'homme, 2009; Ingolfsson & Andersen, 2011; Paxman et al., 2017). Therefore, post-treatment processes for the nanoparticle's suspensions to remove excess organic solvents are essential. Such treatment can be done by dialysis, dilution, centrifugation, or slight heating (Sato et al., 2016; Gdowski et al., 2018; Morikawa et al., 2018; Rocés et al., 2020; Sato et al., 2020).

Overnight dialysis for nanoparticles is the most used process for removing organic solvents after their manufacture using microfluidic devices (Leung et al., 2012; 2015; Hashiba et al., 2020; Younis et al., 2021). Unfortunately, such a method is time-consuming as it takes several hours and may alter the nanoparticles' properties.

Polymeric nanoparticles prepared using acetone as an organic solvent were treated for organic solvent removal either by dialyzing against water for 4 h or by evaporation in a fume hood (Hong et al., 2018). The PS values for nanoparticles subjected to the afore-mentioned post-treatment

processes were 89 and 102 nm, respectively, highlighting the influence of the post-treatment process on the properties of nanoparticles.

Purification of 1,2-dioleoyl-3-trimethylammonium propane (chloride salt) (cationic amino lipid)-based nanoparticles by dialysis against buffer did not change their PS values; however, heptatriaconta-6,9,28,31-tetraen-19-yl 4-(dimethylamino) butanoate (ionizable lipid)-based nanoparticles became more unstable after dialysis. This would suggest the need for the fast removal of the organic solvent in such a formulation to retain its properties (Rocés et al., 2020).

Kimura et al. investigated the effect of the post-treatment process to decrease ethanol content (from 25 to 1% v/v) on the size of the lipid-based nanoparticles by using a microfluidic baffle device and compared such post-treatment process with dialysis or dilution followed by dialysis against buffer (Kimura et al., 2020). It was found that PS values of 1-palmitoyl-2-oleoyl-sn-glycero-3-phosphocholine (POPC)-based nanoparticles post-treated by a simple microfluidic baffle device at FR higher than 10 $\mu\text{L}/\text{min}$ were smaller than those post-treated by dialysis or dilution processes. A similar observation was found for 1,2-dipalmitoyl-sn-glycero-3-phosphocholine and 1,2-distearoyl-sn-glycero-3-phosphoethanolamine-N-[amino(poly-(ethylene glycol))-2000]-based nanoparticles when post-treated by microfluidic baffle device at TFR of 500 $\mu\text{L}/\text{min}$. This was due to the immediate ethanol dilution to 1% v/v within milliseconds using a microfluidic baffle device, opposite to the conventional methods, which consume a long time. On the other hand, POPC/cholesterol-based nanoparticles had almost the same PS values, regardless of the post-treatment method used (Kimura et al., 2020). This may be due to the addition of cholesterol which suppresses the ability of ethanol to develop interdigital structure lipid in the lipid membrane, which cause membrane fusion and an increase in particles size for the obtained particles (De Kruijff et al., 1976).

Tangential flow filtration was used to purify and concentrate solid lipid nanoparticles after microfluidizer homogenization (Anderluzzi et al., 2019). This method involves the recirculation of the sample to be purified across ultrafiltration polymeric membranes for solvent exchange using a pressure-driven purification process. Unlike the conventional dialysis method (dead-end filtration method), membrane fouling is minimized, and a high filtration rate with higher product recovery is maintained. Tangential flow filtration devices can process sample volumes as small as ten milliliters or as large as thousands of liters, potentiating their use in nanoparticles purifications on large scales (Interchim Innovations, 2021; Pall Corporation, 2021).

4. Different types of nanoparticles manufactured using microfluidics

The experimental setup and the nanoparticles composition affect the properties of the produced nanoparticles, which by investigation and analysis could comprehensively clarify the capabilities of microfluidics in the fabrication of nanoparticles.

4.1. Lipid-based nanoparticles

Lipid-based nanoparticles are effective, multipurpose carriers that can be assembled from liquid or solid lipids. Different types of lipids can be used to change the properties of the formulated nanoparticles.

Riewe et al. prepared nanoemulsions and nanoparticles using segmented gas-liquid flow, high-pressure, and staggered herringbone micromixers; and compared their PS and PDI values (Riewe et al., 2020). The feature and operation conditions of the three apparatus are demonstrated in Figure 7. Nanoemulsion and lipid-based nanoparticles were prepared using the investigated micromixers by combining a lipid-containing ethanol solution with an aqueous solution. Nanoemulsion was prepared by mixing 5 mg/mL castor oil in ethanol with 0.278 mg/mL Tween[®] 80 in water or mixing 5 mg/mL castor oil with 2.5 mg/mL Tween[®] 80 in ethanol with water. Lipid-based nanoparticles were fabricated by mixing 10 mg/mL glycerol monooleate in ethanol with 0.222 mg/mL poloxamer 407 in water (Riewe et al., 2020). Results revealed that high-pressure micromixers led to the formation of nanoemulsions and lipid-based nanoparticles with distinctly smaller PS values than that for the corresponding nanoparticles constructed *via* segmented-flow micromixers (Melzig et al., 2019).

In the same study, it was found that the mixing of the ethanolic and aqueous solutions using the NanoAssemblr platform (staggered herringbone micromixers) was influenced by the variation of TFR. Increasing the FR from 2 (Re number \approx 124) to 10 mL/min (Re number \approx 622) resulted in the formation of nanoparticles with a small PS similar to that produced by a high-pressure micromixer. When they were formulated using higher FR, Castor oil nanoemulsions and lipid-based nanoparticles had higher (multimodal) and lower PDI (monomodal).

Although microfluidics has the potential to reduce the PDI-value of the lipid-based nanoparticles, this preparation technology produced bimodal PS distributions (high PDI-value) in case of nanoemulsions prepared by high-pressure micromixers due to the backflow near the nozzles and slow ability of surfactant to stabilize the fast formed particles (Riewe et al., 2020). Also, nanoemulsions had high PDI (multimodal) when they were formulated using the NanoAssemblr platform with high FR. This would highlight that increasing the FR could affect positively or negatively the nanoparticles' size distribution (Riewe et al., 2020).

Several studies highlighted the effect of the lipid concentration on the PS of lipid-based nanoparticles prepared using microfluidic techniques. It was reported that increasing POPC concentration in ethanol solution (5–10, or 20 mg/mL) increased the PS for the obtained nanoparticles from 25 to 80 nm when mixed with saline. This was due to the fusion and formation of large-sized bilayered phospholipid fragments at the saline-ethanol interface during mixing (Maeki et al., 2017). Similar results appeared during the production of solid lipid nanoparticles, where smaller-sized, more uniform nanoparticles (low PDI) were obtained when lower lipid contents in an ethanolic phase were used. Furthermore, the type of the used surfactant added to the aqueous phase

greatly influenced the properties of the produced nanoparticles. Surfactants with low molecular weight as Pluronic F68 was more potent to stabilize the nanoparticles and thus produced nanoparticles with smaller PS than those obtained using polyvinyl alcohol or Pluronic F127 (with higher molecular weight values) (Arduino et al., 2021).

4.2. PLGA-based nanoparticles

PLGA is a biodegradable, biocompatible, and FDA-approved polymer applied extensively in sustained drug release approaches for the incorporation of hydrophilic and lipophilic drugs (Danhier et al., 2012; Masood, 2016).

Although adjusting the FR and the viscosity of the injected fluids influenced the mixing, in a study, the NanoAssemblr system (staggered herringbone micromixers) was utilized to guarantee efficient mixing between the two mixed phases during the preparation of curcumin-loaded PLGA nanoparticles by emulsion solvent dispersion technique (Morikawa et al., 2018). Using passive mixers like staggered herringbone could decrease mixing time (Valencia et al., 2010; Sun et al., 2013) by disturbing the laminar flow and creating chaotic advection (Du et al., 2010; Pattni et al., 2015) to produce homogenous nanoparticles. The study revealed that TFR of the organic phase (PLGA/curcumin in acetone) and aqueous phase (polyvinyl alcohol in water), FRR, and PLGA type affected the PS, PDI, and encapsulation efficiency values for the obtained nanoparticles where the obtained PSs were less than 200 nm by increasing the TFR, on the other hand, the PDI increased. The encapsulation efficiency decreased with this increase in the TFR, indicating the preparation of more homogenous nanoparticles at the slowest TFR (Morikawa et al., 2018). This finding might be due to the higher crystallization rate of curcumin than PLGA. The FRR (organic/aqueous solutions) of 3:1 showed to produce nanoparticles with small PDI while raising the FRR up to 5:1 increased the nanoparticles' PDI. The same increase in nanoparticles PDI was detected by increasing the molecular weight of PLGA used in preparing the nanoparticles from 4000 to 54,000 g/mol, additionally, increasing the PLGA molecular weight up to 17,000 g/mol resulted in decreased nanoparticles encapsulation efficiency, and then an unexpected increase in encapsulation efficiency was recorded for nanoparticles prepared using PLGA with molecular weight more than or equal to 38,000 g/mol. This interesting finding was attributed to the faster crystallization rate of the high molecular weight polymer compared to the drug, hence enhancing drug encapsulation (Habib et al., 2012). The produced nanoparticles were diluted several times post preparation to get rid of the organic solvent, and then they were freeze dried.

A study conducted by Chiesa et al. stated the significant effect of the FRR on the PS of PLGA nanoparticles fabricated using PLGA (75:25; lactic: glycolic acids monomers) employing the NanoAssemblr Benchtop Device (Chiesa et al., 2018).

The benefits gained from the microfluidic approach in the preparation of polymeric nanoparticles necessitating a conjugation chemical reaction were highlighted by Streck et al.

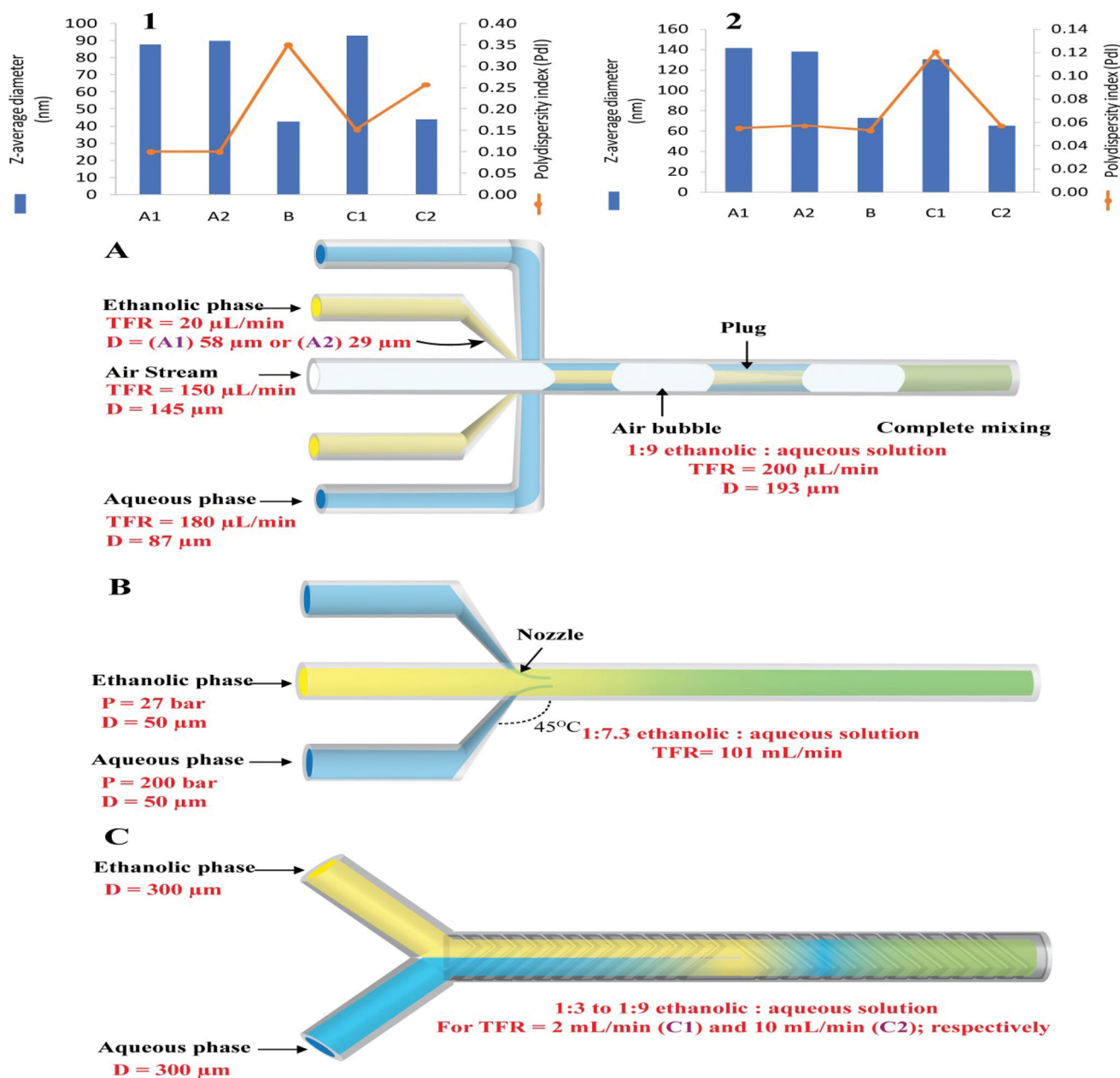


Figure 7. Influence of microfluidic structure and operation conditions on particle size (z-average diameter) and polydispersity index (PDI) of the nanoparticles (Redrawn under permission of Elsevier from reference (Riewe et al., 2020)). (A) Segmented-flow micromixer with large (A1; 58 μm) or small (A2; 29 μm) diameter ethanol channel; (B) High-pressure micromixer and (C) Staggered herringbone micromixer with different TFRs (C1 = 2 or C2 = 10 mL/min) in the mixing channel. The apparatus were used to mix (1) 5 mg/mL castor oil and 2.5 mg/mL polysorbate 80 in ethanol with water or (2) 10 mg/mL glycerol monooleate in ethanol with 0.222 mg/mL poloxamer 407 in water. TFR is total flow rate, D is channel diameter, and P is pressure.

(2019b). The research team succeeded in forming positively charged cell-penetrating peptides (CPP)-coated PLGA nanoparticles using the NanoAssemblr Benchtop Device. These nanoparticles were compared to their counterparts produced using traditional bulk methods. Generally, the production of nanoparticles using the microfluidics was more time-efficient and reproducible, giving particles with size 150 nm and PDI < 0.15 for uncoated particles and slightly larger size particles between 160 and 180 nm for CPP-coated ones with high conjugation efficiency up to 80% (Streck et al., 2019b).

The research team further compared in another research article the post microfluidic conjugation reaction required to prepare (CPP)-tagged PLGA nanoparticles in a NanoAssemblr

Benchtop Device to the *in-situ* microfluidic conjugation reaction (Figure 8). The device was a Y-shaped inlet configuration coupled with a serpentine-shaped microchannel equipped with a staggered herringbone mixer (Streck et al., 2019a). Results revealed that higher FRR (aqueous/organic solutions) produced smaller nanoparticles with less PDI, emphasizing the role of dilution and rapid precipitation of the polymer. TFR and FRR of 10 mL/h and 6:1, respectively, succeeded in producing particles of size around 150 nm and PDI ranging from 0.12 to 0.18. The conjugated nanoparticles produced by post microfluidics did not show CPP distribution throughout the nanoparticles, opposite to those prepared by *in-situ* microfluidics (Streck et al., 2019a). The ability of microfluidics

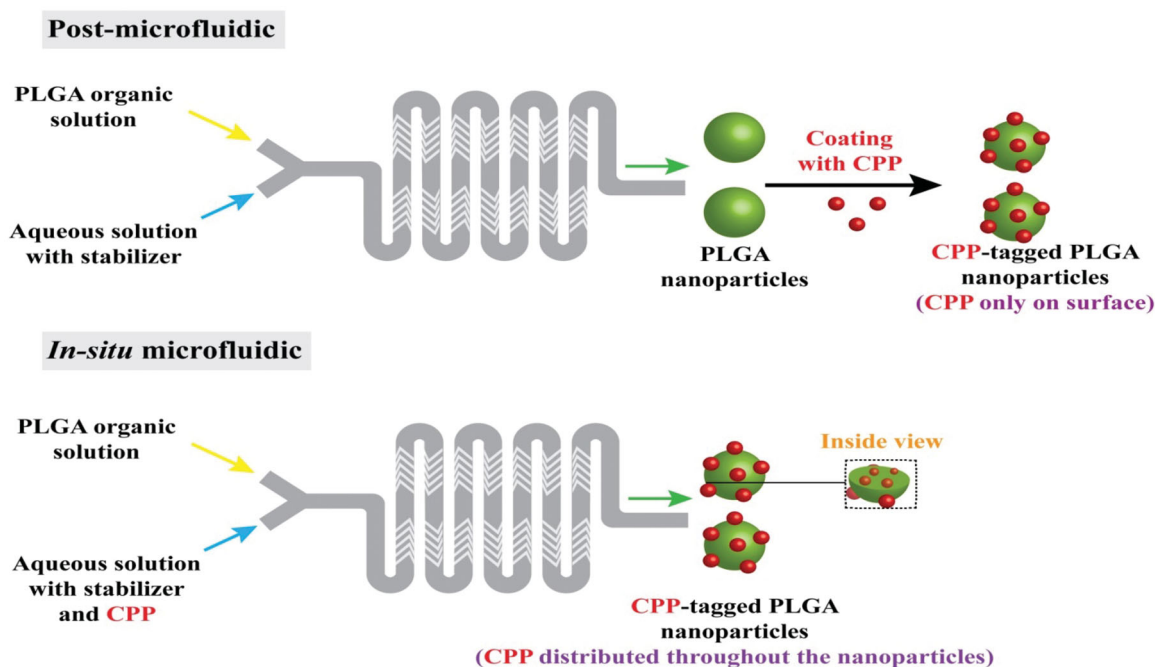


Figure 8. Comparison between A) post microfluidics and B) *in-situ* microfluidic techniques for the preparation of charged cell-penetrating peptides (CPP)-coated PLGA nanoparticles showing the different distribution of CPP through the formed nanoparticles (Redrawn under permission of Elsevier from reference (Streck et al., 2019a)) CPP is charged cell-penetrating peptides.

to prepare reproducible nanoplatforms with the tunable surface could open the door for exploring the nano/biointerface interactions, hence correlating the *in-vitro/in-vivo* behavior of nanoformulations.

PLGA-PEG was used to prepare a library of nanoparticles with different physicochemical properties (size, charge, ligand density, and drug load). Trials aimed at using microfluidics for the preparation of nanoparticles have the ability to evade the macrophages *in-vitro* and *in-vivo* in mice; hence would be suitable for further clinical translation. A multi-inlet mixing unit equipped with a 3D micromixer was utilized for the introduction of different nanoparticles precursors. Different precursors included; PLGA-PEG with different end groups (amine, carboxyl, and methoxy) to impart different charges, different molecular weights for both PLGA (affect size) as well as PEG (affect hydrophilicity), and finally, PLGA-PEG conjugated with *S,S*-2-[3-[5-amino-1-carboxypentyl]uriedo] pentanoic acid as a ligand (in different densities). These precursors were rapidly mixed with an aqueous phase by applying 3D flow-focusing microfluidics (Rhee et al., 2011). A syringe pump for each inlet was used to control the mixing ratio for each precursor aiming at tailoring nanoparticles properties. Results revealed that PS increased from 25 to 200 nm by increasing PLGA molecular weight. Moreover, nanoparticles with different surface charges, positive, negative, or neutral in the case of amine, carboxyl, and methoxy end groups, respectively, were fabricated. As a model drug, Docetaxel was added in different amounts, where the final drug load was varied by altering polymer concentration and using a stream of plain organic solvent to varying the concentration. The fabricated nanoparticles with ligand density approaching 200 ligands per nanoparticle showed minimum recognition by macrophages and maximum uptake by tumor cells (Valencia et al., 2013).

Despite the myriad advantages of fabrication of PLGA-based nanoparticles *via* microfluidics, the entrapment efficiency and drug loading of the produced particles are, to some extent, low. This might be endorsed to the solvent displacement process of the water-miscible solvents into the aqueous phase, which results in the accumulation of PLGA chains and formation of small particles while a big part of the active agents is lost. This obstacle was addressed in one study where a mixture of water-miscible solvents (dimethyl sulfoxide [DMSO] and DCM) was used. DMSO displaced into the water phase while the other solvent (DCM) entrapped the drug particles inside the nanoparticles during formation, hence averting missing a large part of the dose. This assumption was further confirmed by the enhancement of entrapment efficiency as well as drug loading when the proportion of DCM was increased in the solvent mixture (Xu et al., 2017). Eventually, it can be concluded that tailoring the organic solvent mixture can be of great importance in formulating nanoparticles with improved properties.

4.3. Cross-linked nanoparticles

Ionic gelation occurs due to electrostatic interaction between positive and negative charges of cross-linking agents. Flow focusing (cross-junction) microfluidics is one of the most used microfluidics in ionic gelation and cross-linking process. Generally, it consists of three inlets (a middle inlet and two lateral inlets) and one outlet, where the cross-linking agents are streamed in separate side inlets (Moradikhah et al., 2020; Soheili et al., 2021). Aşık and his team studied the effect of microchannel designs (straight and hurdles microchannel), different materials concentrations, inlet solutions pH values, and FR on the properties of chitosan/sodium

tripolyphosphate (TPP) cross-linked nanoparticles. Using the microfluidics with hurdles and high FR (120 mL/h for both chitosan and TPP) produced less aggregated particles with no clogging for microchannels. Chitosan and TPP streamed at pH 4.5 in concentrations of 0.06 and 0.03%, respectively, making nanoparticles with a size value equal to 190 nm (Aşik et al., 2021).

One of the drawbacks in the ionic gelation process in microfluidics is the formation of microfiber-like structures inside the microchannels. This phenomenon occurs due to the rapid electrostatic interaction between the cross-linking agents at the early microchannel regions. To overcome this problem, water streams in the middle channel are used to delay the process of ionic gelation, and this method is called a central aqueous stream system. This process was conducted by Pessoa and his team, which successfully prepared chitosan/adenosine triphosphate (ATP) nanoparticles with PS values < 129 nm and PDI around 0.12. The authors streamed water through the middle inlet while chitosan and ATP were streamed through the lateral inlets of the microfluidic device. The stream of water acted as both a barrier and diffusion layer between chitosan and ATP streams, slowing down the diffusion and delaying the ionic gelation. Additionally, it was found that increasing the FRR (chitosan + ATP/water) reduced the diffusion path width between both chitosan and ATP, resulting in increased PS and formation of microfiber structures at the early regions of mixing as the case with the regular method (Figure 9) (Pessoa et al., 2017).

Alginate nanoparticles cross-linked with calcium chloride through ionic gelation were also prepared using cross-junction microfluidics, where sodium alginate solution was streamed through the central inlet channel, and calcium chloride were streamed through the lateral inlets. The studies showed the fabrication of alginate nanoparticles with PS values < 400 nm (Mahmoodi et al., 2016; Mahmoudi et al., 2020). In another study, a central aqueous stream system was applied to prepare calcium alginate nanoparticles loaded with doxorubicin. The study evaluated the influence of FRR and channel length on PS. Decreasing channel length from 100 to 30 mm showed a reduction in the PS values from 436.5 to 300 nm due to the reduced resident time in a microchannel. On the other hand, the PS values decreased from 514 to 327 nm with decreasing the FRR from 4 to 0.5, as this FRR value supported a suitable diffusion region with a shorter mixing time for alginate and calcium chloride (Cai et al., 2019).

4.4. Miscellaneous nanoparticles

Dual stimuli-responsive nanoparticles with enzyme-responsive ester bonds and oxidation-responsive sulfide linkages were prepared using high-density polyethylene and aqueous stabilizers like Pluronic L-64 and PEG 6000. The main concept relies on the destabilization of nanoparticles under the effect of esterase enzyme and/or oxidation reactions resulting in the controlled release of loaded drugs or biological molecules. Manipulating the microfluidic parameters allowed for the fabrication of nanoparticles with enhanced properties.

Increasing TFR from 2 to 6 mL/min at FRR (aqueous/organic) of 3/1, decreased the PS significantly from 104 to 94 nm with no further change when raised to 12 mL/min. The nanoparticles were monomodal with PDI < 0.1. Moreover, the concentration of nanoparticles affected mostly the size and stability of the produced particles, where smaller and more stable particles with no signs of aggregation over 2 months of storage were produced at nanoparticles concentration of 1 and 4 mg/mL, in contrast, larger and less stable particles were formed at 7 and 14 mg/mL concentrations. The merits of these nanoparticles were obvious when their biological effect on HeLa cells was tested by preparing Nile Red loaded nanoparticles and highlighting the role of the used aqueous stabilizer. PEG stabilized nanoparticles showed concentration-dependent cell viability enhancement, with > 80% viability by increasing PEG concentration > 500 µg/mL. Moreover, the internalization of Nile Red-loaded nanoparticles was considerably higher than free Nile Red (Hong et al., 2018).

In addition to the enzyme and/or reaction-assisted destabilization for nanoparticles, other stimuli-responsive nanoplatforms were fabricated by applying the microfluidic technique. Polymersomes constructed using the pH-responsive poly([N-(2-hydroxypropyl)]-methacrylamide)-b-poly[2-(diisopropylamino)ethyl methacrylate] block copolymers were of due relevance, especially in pathophysiological states distinguished by alterations in physiological pH values like in case of cancer. Polymersomes could introduce a solution for the delivery of hydrophilic therapeutics like the anticancer drug; doxorubicin. Taking into consideration the low pH value of cancer cells (Glunde et al., 2003) as well as the protonation of the copolymer at pH < 6.5, hence polymersomes were self-assembled at pH > 6.8. Increasing the FRR (aqueous/organic) to 200/100 produced smaller-sized particles (≈60 nm) with a small PDI value of 0.06 due to the efficient, rapid mixing being achieved. Drug release data confirmed the disassembly of the polymersomes at pH 5.5, where more than 50% of the drug was released after 4 h. On the other hand, at pH 7.4, a sustained release of the drug was observed, where 90% were released after 48 h (Albuquerque et al., 2019). This rapid release in an acidic environment exhibited consistent bio-distribution and enhanced cellular uptake of the polymersomes by tumor cells compared to the pure drug, which would guarantee selective cytotoxicity when administered *in-vivo*.

For better handling and stability issues, the production of a dry state form of nanoparticles is the best opinion. In one study, coupling of nanoprecipitation *via* micromixers with spray drying was adopted to fabricate dry state ketoprofen-loaded nanoparticles using poly(methyl methacrylate) as a polymer and Cremophor ELP as a surfactant. Impact jet micromixers produced the smallest PS compared to the other used ones; Y-type and high-pressure interdigital multi lamination micromixers which might be attributed to the fast mixing, supersaturation, nucleation, and surfactant adsorption. Moreover, the strong intermeshing of the streamlines in the mixing chamber along with the weak ones in the outlet of the micromixer resulted in the production of small PSs. Spray drying using mannitol post the microfluidic assisted

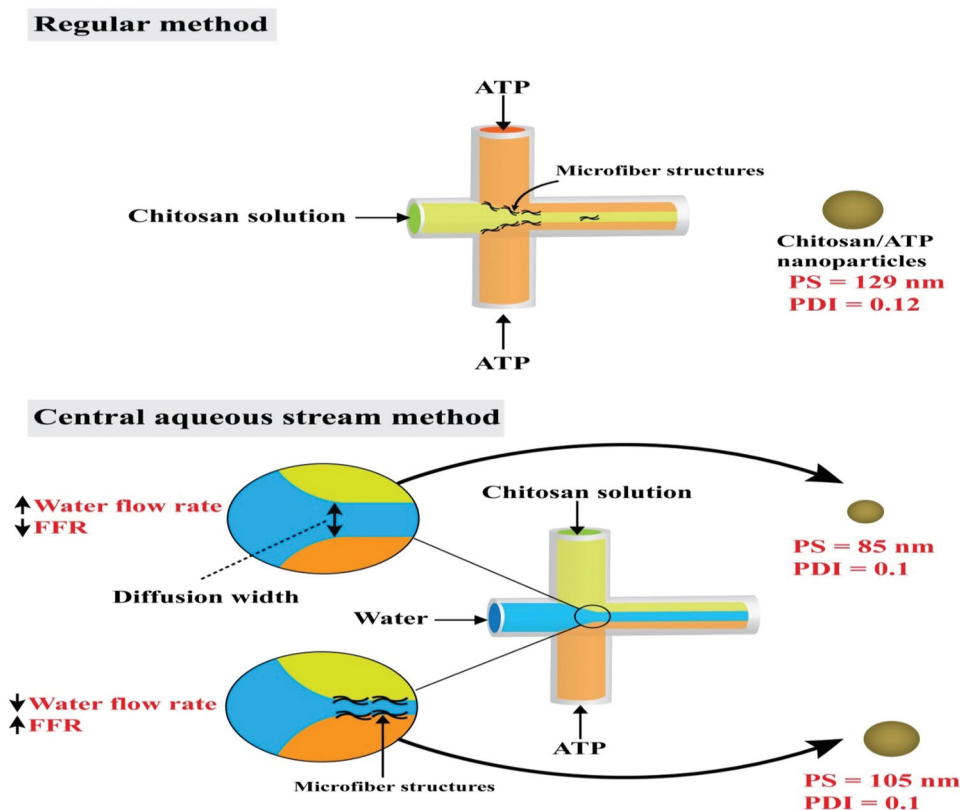


Figure 9. Preparation of chitosan/ATP nanoparticles by ionic gelation *via* regular and central aqueous stream microfluidic methods. The figure shows the effect of the conducted methods on the particle size (PS) and polydispersity index (PDI) (Data in this figure was obtained from Pessoa et al. (2017)).

nanoprecipitation altered neither the PS nor the PDI-values; however, a significant lower drug release rate (10% less) was obtained with re-dispersed spray-dried particles compared to the non-spray dried ones which might be endorsed to the smaller entrapment efficiency (Ding et al., 2019). Varying the operating conditions could produce tunable, reproducible nanoparticles for any certain purpose.

5. Scale-up production for nanoparticles using microfluidics

Optimization of the microfluidic platform design, solvents, and FR can generate particles with constant and stable production quality (Utada et al., 2005; Shum et al., 2008). Unlike traditional methods for nanoparticles fabrications, the microfluidic technique may offer a reproducible and continuous nanofabrication platform to scale-up nanoparticle production, which potentiates transferring this technique to the industrial scale.

One of the proposed techniques to increase the produced sample sizes in microfluidic systems is by parallelizing several microfluidic channels or lengthening the production runs (Lier et al., 2018). Belliveau et al. produced POPC/cholesterol-based nanoparticles loaded with small interfering RNA (siRNA) using six parallel herringbone micromixers (Belliveau et al., 2012). This system was able to produce nanoparticles at an FR of 72 mL/min. According to the PEG-lipid content, the nanoparticles had a controlled size of over 20–100 nm,

whereby siRNA was encapsulated with efficiencies reaching 100%. In another study, eight parallel microfluidic mixers were successfully designed under cGMP conditions to produce lipid-based nanoparticles loaded with RNA at a production rate of 25 L per 4 h.

The operated FR in microfluidics can control the nanoparticles production output. Lipid-based nanoparticles fabricated using segmented gas-liquid flow, high-pressure, and staggered herringbone micromixers (Figure 7) were produced under TFR of 200 μ L/min, 101 mL/min, and 2 mL/min or 10 mL/min; respectively (Riewe et al., 2020). Both herringbone and high-pressure micromixers generated particles with similar size values. However, high-pressure micromixers succeeded in giving higher production quantities of 101 mL/min compared to herringbone micromixers (10 mL/min). This would suggest the possibility of using a high-pressure micromixer as a high-throughput microfluidic system (Riewe et al., 2020), as it can be operated for a short time in order to obtain appropriate quantities.

Ionizable lipid mix (GenVoy-ILM™)-based nanoparticles loaded with polyadenylic acid was produced using toroidal microfluidics (Roces et al., 2020). The microfluidic device was operated at TFR of 12, 60, and 200 mL/min. The nanoparticles showed comparable sizes (around 78 nm) with high polyadenylic acid encapsulation efficiencies (larger than 95%). Also, the same microfluidic device was used to prepare protein (ovalbumin)-loaded liposomes in operation rate values of 1, 12, and 200 mL/min (Webb et al., 2020). The obtained

liposomes had comparable PS values of 60–70 nm with PDI around 0.2 across the tested three FR, indicating this microfluidic technology's scalability.

Liposomes loaded with verteporfin were manufactured using NanoAssemblr™ Benchtop (1–15 mL FR) and scaled ten times *via* the NanoAssemblr Blaze™ (10 mL–1 L FR). The particles produced using both apparatuses had similar PS, PDI < 0.2, and encapsulation efficiency >80% (Brown et al., 2017).

6. Innovative strategies for the preparation of micro/nanofluidic drug delivery systems

Chronic diseases impose an escalating burden on the health care sector, accounting for 75% of medical expenditures on episodic control rather than disease management (Raghupathi & Raghupathi, 2018). Additionally, the idea of using a one-size formulation fitting all patients is not convenient in chronic diseases management. Pediatrics, geriatrics, and disabled patients also require special treatment to enhance their adherence to their therapy. Implantable drug delivery systems could introduce a good solution (Abdel-Salam et al., 2020; Kamel et al., 2020; Eldeeb et al., 2022) to avoid fluctuating drug levels and sustain its release, hence increasing therapeutic effect and patient compliance (Ainslie & Desai, 2008; Elkasabgy & Mahmoud, 2019). Transdermal drug delivery systems, such as microneedles are designed to deliver the skin through the bloodstream (Alkilani et al., 2015). Microneedles and implantable systems could provide several drug release patterns, i.e. zero-order, pulsatile, and on-demand dosing.

A stereolithography 3D printer was used to fabricate combined spiral microfluidics and hollow microneedle resin architecture in dimensions of $1.5 \times 1.2 \times 3.1 \text{ cm}^3$ (Yeung et al., 2019). The microneedles were designed in a pyramidal shape with a triangular base or tip orthogonally aligned with a vertex base. The microfluidics has three inlets connected to a spiral chamber for mixing the solvents, and it is connected to the hollow microneedles (outlets). The hollow syringe-shaped microneedle could comfortably penetrate the human stratum corneum, which ensures drug delivery through a 'poke-and-flow' mode of operation. Furthermore, injecting fluids through the microfluidic three inlets (FR 100 $\mu\text{L}/\text{min}$) achieved homogenized mixing at the outlet. Such a device can be programmed for on-demand synthesis and delivery of nanoparticles through the skin.

Nanofluidic could offer a solution for controlling chronic diseases through the fabrication of miniaturized systems capable of regulating the drug release for long periods of time (Ferrati et al., 2013; Fine et al., 2013). Remote drug release control adds excellent value to the use of implantable systems. Microchip (Santini et al., 1999) is an example, equipped with 20 drug reservoirs (600 nanoliters) and operated wirelessly. Microchip passed the 1st clinical trial in treating women with osteoporosis (EudraCT, number 2010-020040-35) (Farra et al., 2012).

The release of two drugs, methotrexate, and enalapril, administered for the treatment of rheumatoid arthritis was attempted using an implantable system coupled with

nanochannels and operated under the effect of electric current, with modified intensity, for on-demand release (Di Trani et al., 2019). The implant consisted of a silicone nanofluidic membrane, platinum electrodes, drug reservoir, battery, and printed circuit board. The study revealed that the type of platinum electrodes (foil electrodes attached to the nanofluidic membrane or sputtered electrodes) along with the voltage type (positive or negative) affected the drug release. By applying a negative voltage, a decrease in the drug release was observed, confirming the scenario of the movement of particles in certain fluids under the effect of electric current. An opposite effect was obtained with a positive voltage, which was attributed to the fact that both drugs are negatively ionized in physiological pH. Sputtered electrodes offered less reproducible control on the release of the drug compared to the foil electrodes due to the smaller distance between the sputtered electrode and the membrane. The fabricated implant safety was tested *in-vivo* in rats and non-human primates. Results indicated good biological relevance with mild transit inflammation adjacent to the electrodes. Future investigations require finding high-density batteries for a longer lifespan or electrostatic gates controlling the electric current (Bruno et al., 2016; Kim et al., 2018).

From a safety point of view, a switch-off implantable device is of great importance. However, limited options are available to manipulate the drug release in case of any adverse reactions after implantation, imposing the surgical intervention as the sole solution to save the patient. Of course, this procedure is costly and time-consuming. A non-invasive way out of this problem is highly required to deactivate the implantable system and halt the drug release hastily, without training personnel. In this context, nanofluidic-based drug delivery implants coupled with the magnetically activated switch-off micro gates were fabricated (Farina et al., 2017).

The switch-off system was a polymer/metal sandwich. In brief, a stainless-steel mesh (acting as a heating layer) was embedded between two polymer layers (polycaprolactone [PCL]); each with five orifices is forming a sandwich. The switch-off system was incorporated at the port of the implantable delivery device which is composed of a drug reservoir, polyether ether ketone cap (PEEK), and silicone membrane featuring nanochannels to regulate the drug release. The switch-off system was placed between the cap and the silicone membrane. Based on computer simulations, the optimum magnetic field required (FDA approved) to heat the stainless-steel mesh enough to melt the PCL layers was selected, aiming at blocking the drug release. The success of this approach was monitored when the release of rhodamine B dropped by 98 and 90% when tested *in-vitro* and *ex-vivo* (implanted in the dorsum of a cadaveric mouse) correspondingly. This innovative system could help a lot in allergic reactions to any released compound. However, one of the disadvantages of this approach is the complete destruction of the mesh and the impossibility to re-switch the device again (Farina et al., 2017). Exploiting intelligent shape memory polymers, which can alter their shapes under stress and restore them when released, can be a solution. Shape

memory materials can be humidity, temperature, electrical, magnetic, and light-responsive (Elkasabgy & Mahmoud, 2019). Further modifications in the device require re-designing of the implant as well as using thermal isolating materials to reduce the thermal tissue adverse effects.

Nanofluidic implants with tunable drug release introduce a versatile technology for treating infinite ailments. Further developments for these systems should be applied by equipping the implantable systems with micromixers to combine the benefits of preparing drug-loaded nanoparticles *in-situ* and delivering them on-demand in a safe manner.

7. Conclusion and future prospects

This review introduced a comprehensive overview of microfluidic techniques, platforms, and applications in the fabrication of different nanoplatforms, emphasizing its great role in the pharmaceutical and drug delivery field. Microfluidics is a technology with deepened roots in nanoparticle fabrication, presenting several applications mainly related to low cost, high throughput, tunable PS, and excellent batch-to-batch reproducibility. Additionally, microfluidic platforms are not bulky, requiring no large industrial spaces.

Microfluidic platforms or systems can be designed and classified according to the nature of the fabricated nanoparticles as well as the formation technique into; continuous or segmented flow systems. Continuous flow is the most popular, simple technique depending on mixing different liquid phases by diffusion. On the other hand, segmented flow offers a good solution for fabricating nanoparticles requiring reactions by slugs generation without raising the size or complexity of the system. The review threw light on the utilization of micromixers (passive or active) to augment the mixing process. Several types of micromixers were discussed in detail.

Approaches to achieve efficient microfluidics were discussed; as surface modification of the microchannels to enhance the flow besides maintaining the integrity of the channels, anti-fouling effect as a solution to avoid adsorption of particles onto the walls, and finally, post-microfluidic treatment as a way to remove all organic solvents used in the formation of nanoparticles to ensure the stability of the final product.

The fabrication principles of lipid-, PLGA-, and cross-linked based nanoparticles as well as the physicochemical properties of the formed nanoparticles, were presented and discussed. Stimuli-responsive nanoparticles were also displayed.

Regarding scaling-up production using microfluidics, parallelization of several microfluidic channels appeared to be the most used method.

Novel strategies for applying micro/nanofluidic in the drug delivery field highlighted the significance of those techniques in controlling chronic diseases, regulating the drug release for long periods of time, and offering platforms capable of delivering the drug on-demand.

This review suggests the implementation of vast investigational studies to augment the application of microfluidics in nanomedicine to decrease the expenditures of traditional

nanoparticles fabrication methods and warrant the reproducibility of the formed batches. In conclusion, microfluidics is considered the future of nanomedicine.

Disclosure statement

The authors declare that they have no known competing financial interests or personal relationships that could have appeared to influence the work reported in this article.

Funding

The author(s) reported there is no funding associated with the work featured in this article.

Data availability statement

Data is available within the article.

References

- Abate AR, Lee D, Do T, et al. (2008). Glass coating for PDMS microfluidic channels by sol-gel methods. *Lab Chip* 8:1549–8.
- Abdel-Salam FS, Elkheshen SA, Mahmoud AA, et al. (2020). In-situ forming chitosan implant-loaded with raloxifene hydrochloride and bio-active glass nanoparticles for treatment of bone injuries: Formulation and biological evaluation in animal model. *Int J Pharm* 580:119213.
- Abou-Hassan A, Dufreche JF, Sandre O, et al. (2009). Fluorescence confocal laser scanning microscopy for pH mapping in a coaxial flow microreactor: application in the synthesis of superparamagnetic nanoparticles. *J Phys Chem C* 113:18097–105.
- Adel IM, ElMeligy MF, Abdelrahim MEA, et al. (2021). Design and characterization of spray-dried proliposomes for the pulmonary delivery of curcumin. *Int J Nanomedicine* 16:2667–87.
- Ahmed H, Stokke BT. (2021). Fabrication of monodisperse alginate micro-gel beads by microfluidic picoinjection: a chelate free approach. *Lab Chip* 21:2232–43.
- Ainslie KM, Desai TA. (2008). Microfabricated implants for applications in therapeutic delivery, tissue engineering, and biosensing. *Lab Chip* 8: 1864–78.
- Akhter KF, Mumin MA, Lui EMK, et al. (2019). Immunoengineering with ginseng polysaccharide nanobiomaterials through oral administration in mice. *ACS Biomater Sci Eng* 5:2916–25.
- Akther F, Yakob SB, Nguyen N-T, et al. (2020). Surface modification techniques for endothelial cell seeding in PDMS microfluidic devices. *Biosensors* 10:182.
- Al-Ahmady ZS, Donno R, Gennari A, et al. (2019). Enhanced intraliposomal metallic nanoparticle payload capacity using microfluidic-assisted self-assembly. *Langmuir* 35:13318–31.
- Albuquerque LJC, Sincari V, Ja Ger A, et al. (2019). Microfluidic-assisted engineering of quasi-monodisperse pH-responsive polymersomes toward advanced platforms for the intracellular delivery of hydrophilic therapeutics. *Langmuir* 35:8363–72.
- Alkilani AZ, McCrudden MT, Donnelly RF. (2015). Transdermal drug delivery: innovative pharmaceutical developments based on disruption of the barrier properties of the stratum corneum. *Pharmaceutics* 7: 438–70.
- Anderluzzi G, Lou G, Su Y, et al. (2019). Scalable manufacturing processes for solid lipid nanoparticles. *Pharm Nanotechnol* 7:444–59.
- Anna SL, Bontoux N, Stone HA. (2003). Formation of dispersions using “flow focusing” in microchannels. *Appl Phys Lett* 82:364–6.
- Ansari MA, Kim KY, Kim SM. (2018). Numerical and experimental study on mixing performances of simple and vortex micro T-mixers. *Micromachines* 9:204.

- Arduino I, Liu Z, Rahikkala A, et al. (2021). Preparation of cetyl palmitate-based PEGylated solid lipid nanoparticles by microfluidic technique. *Acta Biomater* 121:566–78.
- Aşık MD, Kaplan M, Çetin B, et al. (2021). Synthesis of iron oxide core chitosan nanoparticles in a 3D printed microfluidic device. *J Nanopart Res* 23:1–11.
- Bains A, Cao Y, Kly S, et al. (2017). Controlling structure and function of polymeric drug delivery nanoparticles using microfluidics. *Mol Pharm* 14:2595–606.
- Baret JC. (2012). Surfactants in droplet-based microfluidics. *Lab Chip* 12: 422–33.
- Bashir M, Bashir S, Khan H. (2018). Deposition of polyacrylic acid films on PDMS substrate in dielectric barrier corona discharge at atmospheric pressure. *Surf Interface Anal* 50:879–88.
- Basova EY, Foret F. (2015). Droplet microfluidics in (bio)chemical analysis. *Analyst* 140:22–38.
- Beebe DJ, Mensing GA, Walker GM. (2002). Physics and applications of microfluidics in biology. *Annu Rev Biomed Eng* 4:261–86.
- Belliveau NM, Huft J, Lin PJ, et al. (2012). Microfluidic synthesis of highly potent limit-size lipid nanoparticles for in vivo delivery of siRNA. *Mol Ther Nucleic Acids* 1:e37.
- Bringer MR, Gerdts CJ, Song H, et al. (2004). Microfluidic systems for chemical kinetics that rely on chaotic mixing in droplets. *Philos Transact A Math Phys Eng Sci* 362:1087–104.
- Brown A, Ma, B. Versteeg R, et al. (2017). Manufacture of verteporfin loaded liposomes using a scalable microfluidic platform. Vancouver, Canada: Precision NanoSystems.
- Bruno G, Canavese G, Liu X, et al. (2016). The active modulation of drug release by an ionic field effect transistor for an ultra-low power implantable nanofluidic system. *Nanoscale* 8:18718–25.
- Cai S, Shi H, Li G, et al. (2019). 3D-printed concentration-controlled microfluidic chip with diffusion mixing pattern for the synthesis of alginate drug delivery microgels. *Nanomaterials* 9:1451.
- Cai G, Xue L, Zhang H, et al. (2017). A review on micromixers. *Micromachines* 8:274.
- Capretto L, Cheng W, Hill M, Zhang X. (2011). Micromixing within microfluidic devices. *Microfluidics* 304:27–68.
- Carvalho BG, Ceccato BT, Michelon M, et al. (2022). Advanced microfluidic technologies for lipid nano-microsystems from synthesis to biological application. *Pharmaceutics* 14:141.
- Cejas CM, Monti F, Truchet M, et al. (2018). Universal diagram for the kinetics of particle deposition in microchannels. *Phys Rev E* 98: 062606.
- Chango A, Abdennebi-Najar L, Tessier F, et al. (2006). Quantitative methylation-sensitive arbitrarily primed PCR method to determine differential genomic DNA methylation in Down Syndrome. *Biochem Biophys Res Commun* 349:492–6.
- Chen G, Liu X, Li S, et al. (2018). A droplet energy harvesting and actuation system for self-powered digital microfluidics. *Lab Chip* 18: 1026–34.
- Chiesa E, Dorati R, Modena T, et al. (2018). Multivariate analysis for the optimization of microfluidics-assisted nanoprecipitation method intended for the loading of small hydrophilic drugs into PLGA nanoparticles. *Int J Pharm* 536:165–77.
- Choi CH, Lee H, Weitz DA. (2018). Rapid patterning of PDMS microfluidic device wettability using syringe-vacuum-induced segmented flow in nonplanar geometry. *ACS Appl Mater Interfaces* 10:3170–4.
- Chou WL, Lee PY, Yang CL, et al. (2015). Recent advances in applications of droplet microfluidics. *Micromachines* 6:1249–71.
- Clark I, Dunne PW, Gomes RL, et al. (2017). Continuous hydrothermal synthesis of Ca2Al-NO3 layered double hydroxides: the impact of reactor temperature, pressure and NaOH concentration on crystal characteristics. *J Colloid Interface Sci* 504:492–9.
- Cui F, Jafarishad H, Zhou Z, et al. (2020). Batch fabrication of electrochemical sensors on a glycol-modified polyethylene terephthalate-based microfluidic device. *Biosens Bioelectron* 167:112521.
- Damiati S, Kompella U, Damiati S, et al. (2018). Microfluidic devices for drug delivery systems and drug screening. *Genes* 9:103.
- Danhier F, Ansorena E, Silva JM, et al. (2012). PLGA-based nanoparticles: an overview of biomedical applications. *J Control Release* 161:505–22.
- De BS, Singh A, Elias A, et al. (2020). An electrochemical neutralization energy-assisted membrane-less microfluidic reactor for water electrolysis. *Sustain Energy Fuels* 4:6234–44.
- de Carvalho BG, Taketa TB, Garcia BBM, et al. (2021). Hybrid microgels produced via droplet microfluidics for sustainable delivery of hydrophobic and hydrophilic model nanocarriers. *Mater Sci Eng C Mater Biol Appl* 118:111467.
- De Kruijff B, Cullis PR, Radda GK. (1976). Outside-inside distributions and sizes of mixed phosphatidylcholine-cholesterol vesicles. *Biochim Biophys Acta* 436:729–40.
- Demello AJ. (2006). Control and detection of chemical reactions in microfluidic systems. *Nature* 442:394–402.
- Deng B, Ruiter JD, Schröen K. (2019). Application of microfluidics in the production and analysis of food foams. *Foods* 8:476.
- Deshmukh AA, Liepmann D, Pisano AP. (2001). Characterization of a micro-mixing, pumping, and valving system. *Transducers' 01 Eurosensors XV*. Berlin, Germany: Springer, 922–5.
- Di Trani N, Silvestri A, Bruno G, et al. (2019). Remotely controlled nanofluidic implantable platform for tunable drug delivery. *Lab Chip* 19: 2192–204.
- Dietzel A. (2016). *Microsystems for pharmatechnology*. Vol. 1007. Cham, Switzerland: Springer, 978–3.
- Ding S, Serra CA, Anton N, et al. (2019). Production of dry-state ketoprofen-encapsulated PMMA NPs by coupling micromixer-assisted nanoprecipitation and spray drying. *Int J Pharm* 558:1–8.
- Du Y, Zhang Z, Yim CHO, et al. (2010). A simplified design of the staggered herringbone micromixer for practical applications. *Biomicrofluidics* 4:024105.
- Duraiswamy S, Khan SA. (2009). Droplet-based microfluidic synthesis of anisotropic metal nanocrystals. *Small* 5:2828–34.
- Ehrfeld W, Golbig K, Hessel V, et al. (1999). Characterization of mixing in micromixers by a test reaction: single mixing units and mixer arrays. *Ind Eng Chem Res* 38:1075–82.
- Eldeeb AE, Salah S, Mabrouk M, et al. (2022). Dual-drug delivery via zein in situ forming implants augmented with titanium-doped bioactive glass for bone regeneration: preparation, in vitro characterization, and in vivo evaluation. *Pharmaceutics* 14:274.
- Elkasabgy NA, Mahmoud AA. (2019). Fabrication strategies of scaffolds for delivering active ingredients for tissue engineering. *AAPS PharmSciTech* 20:1–18.
- Endaylalu SA, Tien WH. (2022). A numerical investigation of the mixing performance in a Y-junction microchannel induced by acoustic streaming. *Micromachines* 13:338.
- Erbacher C, Bessoth FG, Busch M, et al. (1999). Towards integrated continuous-flow chemical reactors. *Microchim Acta* 131:19–24.
- Erdem K, Ahmadi VE, Kosar A, et al. (2020). Differential sorting of micro-particles using spiral microchannels with elliptic configurations. *Micromachines* 11:412.
- Erfle P, Riewe J, Bunjes H, et al. (2017). Optically monitored segmented flow for controlled ultra-fast mixing and nanoparticle precipitation. *Microfluid Nanofluid* 21:179.
- Erfle P, Riewe J, Bunjes H, et al. (2019). Stabilized production of lipid nanoparticles of tunable size in Taylor flow glass devices with high-surface-quality 3D microchannels. *Micromachines* 10:220.
- Farina M, Ballerini A, Torchio G, et al. (2017). Remote magnetic switch off microgate for nanofluidic drug delivery implants. *Biomed Microdevices* 19:42.
- Farra R, Sheppard NF, McCabe L, et al. (2012). First-in-human testing of a wirelessly controlled drug delivery microchip. *Sci Trans Med* 4: 122ra21.
- Feng J, Yuan J, Cho SK. (2015). Micropropulsion by an acoustic bubble for navigating microfluidic spaces. *Lab Chip* 15:1554–62.
- Ferrati S, Fine D, You J, et al. (2013). Leveraging nanochannels for universal, zero-order drug delivery in vivo. *J Control Release* 172:1011–9.
- Ferraz M, Nagashima J, Venzac B, et al. (2020). 3D printed mold leachates in PDMS microfluidic devices. *Sci Rep* 10:1–9.
- Fick A. (1855). Ueber diffusion. *Ann Phys Chem* 170:59–86.
- Fine D, Grattoni A, Goodall R, et al. (2013). Silicon micro- and nanofabrication for medicine. *Adv Healthc Mater* 2:632–66.

- Fu Y, Zhou H, Jia C, et al. (2017). A microfluidic chip based on surfactant-doped polydimethylsiloxane (PDMS) in a sandwich configuration for low-cost and robust digital PCR. *Sens Actuatur B* 245:414–22.
- Fujii T, Sando Y, Higashino K, et al. (2003). A plug and play microfluidic device. *Lab Chip* 3:193–7.
- Gao K, Liu J, Fan Y, et al. (2019). Ultra-low-cost fabrication of polymer-based microfluidic devices with diode laser ablation. *Biomed Microdevices* 21:1–7.
- Gdowski A, Johnson K, Shah S, et al. (2018). Optimization and scale up of microfluidic nanolipomer production method for preclinical and potential clinical trials. *J Nanobiotechnol* 16:12.
- Glasgow I, Aubry N. (2003). Enhancement of microfluidic mixing using time pulsing. *Lab Chip* 3:114–20.
- Glunde K, Guggino SE, Solaiyappan M, et al. (2003). Extracellular acidification alters lysosomal trafficking in human breast cancer cells. *Neoplasia* 5:533–45.
- Gobby D, Angeli P, Gavriilidis A. (2001). Mixing characteristics of T-type microfluidic mixers. *J Micromech Microeng* 11:126–32.
- Gonidec M, Puigmartí-Luis J. (2018). Continuous-versus segmented-flow microfluidic synthesis in materials science. *Crystals* 9:12.
- Günther A, Jensen KF. (2006). Multiphase microfluidics: from flow characteristics to chemical and materials synthesis. *Lab Chip* 6:1487–503.
- Gunther A, Jhunjhunwala M, Thalmann M, et al. (2005). Micromixing of miscible liquids in segmented gas-liquid flow. *Langmuir* 21:1547–55.
- Gunther A, Khan SA, Thalmann M, et al. (2004). Transport and reaction in microscale segmented gas-liquid flow. *Lab Chip* 4:278–86.
- Habib SM, Amr AS, Hamadneh IM. (2012). Nanoencapsulation of alpha-linolenic acid with modified emulsion diffusion method. *J Am Oil Chem Soc* 89:695–703.
- Hamblin MR, Karimi M. (2020). *Biomedical applications of microfluidic devices*. Cambridge (MA): Academic Press.
- Hamdallah SI, Zoqlam R, Erfle P, et al. (2020). Microfluidics for pharmaceutical nanoparticle fabrication: the truth and the myth. *Int J Pharm* 584:119408.
- Harrison DJ, Manz A, Fan Z, et al. (1992). Capillary electrophoresis and sample injection systems integrated on a planar glass chip. *Anal Chem* 64:1926–32.
- Hashiba A, Toyooka M, Sato Y, et al. (2020). The use of design of experiments with multiple responses to determine optimal formulations for in vivo hepatic mRNA delivery. *J Control Release* 327:467–76.
- He Y, Kim KJ, Chang CH. (2020). Segmented microfluidic flow reactors for nanomaterial synthesis. *Nanomaterials* 10:1421.
- Hiltunen J, Liedert C, Hiltunen M, et al. (2018). Roll-to-roll fabrication of integrated PDMS-paper microfluidics for nucleic acid amplification. *Lab Chip* 18:1552–9.
- Hong SH, Patel T, Ip S, et al. (2018). Microfluidic assembly to synthesize dual enzyme/oxidation-responsive polyester-based nanoparticulates with controlled sizes for drug delivery. *Langmuir* 34:3316–25.
- Hu X, Yang F, Guo M, et al. (2020). Fabrication of polyimide microfluidic devices by laser ablation based additive manufacturing. *Microsyst Technol* 26:1573–83.
- Ingolfsson HI, Andersen OS. (2011). Alcohol's effects on lipid bilayer properties. *Biophys J* 101:847–55.
- Interchim Innovations. (2021). KrosFlo hollow fiber ultrafiltration modules. Product data sheet Available at: <https://www.interchim.com/> [cited 11 March 2021].
- Jahangiri F, Hakala T, Jokinen V. (2020). Long-term hydrophilization of polydimethylsiloxane (PDMS) for capillary filling microfluidic chips. *Microfluid Nanofluid* 24:1–11.
- Jamalabadi MYA, DaqiqShirazi M, Kosar A, et al. (2017). Effect of injection angle, density ratio, and viscosity on droplet formation in a microfluidic T-junction. *Theor Appl Mech Lett* 7:243–51.
- Jung SY, Park JE, Kang TG, et al. (2019). Design optimization for a microfluidic crossflow filtration system incorporating a micromixer. *Micromachines* 10:836.
- Kajtez J, Buchmann S, Vasudevan S, et al. (2020). 3D-Printed soft lithography for complex compartmentalized microfluidic neural devices. *Adv Sci (Weinh)* 7:2001150.
- Kamel R, El-Wakil NA, Abdelkhalik AA, et al. (2020). Nanofibrillated cellulose/cyclodextrin based 3D scaffolds loaded with raloxifene hydrochloride for bone regeneration. *Int J Biol Macromol* 156:704–16.
- Kang X, Luo C, Wei Q, et al. (2013). Mass production of highly monodisperse polymeric nanoparticles by parallel flow focusing system. *Microfluid Nanofluid* 15:337–45.
- Khan SA, Jensen KF. (2007). Microfluidic synthesis of Titania shells on colloidal silica. *Adv Mater* 19:2556–60.
- Khan IU, Serra CA, Anton N, et al. (2015). Production of nanoparticle drug delivery systems with microfluidics tools. *Expert Opin Drug Deliv* 12:547–62.
- Khemthongcharoen N, Uawithya P, Chanasakulniyom M, et al. (2021). Polydimethylsiloxane (PDMS) microfluidic modifications for cell-based immunofluorescence assay. *J Adhes Sci Technol* 35:955–18.
- Kim J, Cho H, Kim J, et al. (2021). A disposable smart microfluidic platform integrated with on-chip flow sensors. *Biosens Bioelectron* 176:112897.
- Kim S, Kim J, Joung YH, et al. (2019). Optimization of selective laser-induced etching (SLE) for fabrication of 3D glass microfluidic device with multi-layer micro channels. *Micro and Nano Syst Lett* 7:1–7.
- Kim S, Ozalp EI, Darwish M, et al. (2018). Electrically gated nanoporous membranes for smart molecular flow control. *Nanoscale* 10:20740–7.
- Kimura N, Maeki M, Sato Y, et al. (2020). Development of a microfluidic-based post-treatment process for size-controlled lipid nanoparticles and application to siRNA delivery. *ACS Appl Mater Interfaces* 12:34011–20.
- Knight JB, Vishwanath A, Brody JP, et al. (1998). Hydrodynamic focusing on a silicon chip: mixing nanoliters in microseconds. *Phys Rev Lett* 80:3863–6.
- Kotz F, Mader M, Dellen N, et al. (2020). Fused deposition modeling of microfluidic chips in polymethylmethacrylate. *Micromachines* 11:873.
- Krishna KS, Li Y, Li S, et al. (2013). Lab-on-a-chip synthesis of inorganic nanomaterials and quantum dots for biomedical applications. *Adv Drug Deliv Rev* 65:1470–95.
- Kumar V, Prud'homme RK. (2009). Nanoparticle stability: processing pathways for solvent removal. *Chem Eng Sci* 64:1358–61.
- Lauri J, Liedert C, Kokkonen A, et al. (2019). Effect of solvent lamination on roll-to-roll hot-embossed PMMA microchannels evaluated by optical coherence tomography. *Mater Res Express* 6:075333.
- Lee CY, Chang CL, Wang YN, et al. (2011). Microfluidic mixing: a review. *Int J Mol Sci* 12:3263–87.
- Leung AKK, Hafez IM, Baoukina S, et al. (2012). Lipid nanoparticles containing siRNA synthesized by microfluidic mixing exhibit an electron-dense nanostructured core. *J Phys Chem C Nanomater Interfaces* 116:18440–50.
- Leung AKK, Tam YYC, Chen S, et al. (2015). Microfluidic mixing: a general method for encapsulating macromolecules in lipid nanoparticle systems. *J Phys Chem B* 119:8698–706.
- Li J, Carney RP, Liu R, et al. (2018). Microfluidic print-to-synthesis platform for efficient preparation and screening of combinatorial peptide microarrays. *Anal Chem* 90:5833–40.
- Lier S, Riese J, Cvetanoska G, et al. (2018). Innovative scaling strategies for a fast development of apparatuses by modular process engineering. *Chem Eng Process* 123:111–25.
- Li Y, Lee RJ, Huang X, et al. (2017). Single-step microfluidic synthesis of transferrin-conjugated lipid nanoparticles for siRNA delivery. *Nanomedicine* 13:371–81.
- Li Y, Motschman JD, Kelly ST, et al. (2020). Injection molded microfluidics for establishing high-density single cell arrays in an open hydrogel format. *Anal Chem* 92:2794–801.
- Lin TY, Do T, Kwon P, et al. (2017). 3D printed metal molds for hot embossing plastic microfluidic devices. *Lab Chip* 17:241–7.
- Liu R, Chu C-H, Wang N, et al. (2019). Combinatorial immunophenotyping of cell populations with an electronic antibody microarray. *Small* 15:1904732.
- Liu D, Cito S, Zhang Y, et al. (2015). A versatile and robust microfluidic platform toward high throughput synthesis of homogeneous nanoparticles with tunable properties. *Adv Mater* 27:2298–304.

- Liu RH, Stremler MA, Sharp KV, et al. (2000). Passive mixing in a three-dimensional serpentine microchannel. *J Microelectromech Syst* 9: 190–7.
- Löb P, Drese KS, Hessel V, et al. (2004). Steering of liquid mixing speed in interdigital micro mixers—from very fast to deliberately slow mixing. *Chem Eng Technol* 27:340–5.
- Long H, Lai C, Chung CK. (2017). Polyethylene glycol coating for hydrophilicity enhancement of polydimethylsiloxane self-driven microfluidic chip. *Surf Coat Technol* 320:315–9.
- Lorenz T, Bojko S, Bunjes H, et al. (2018). An inert 3D emulsification device for individual precipitation and concentration of amorphous drug nanoparticles. *Lab Chip* 18:627–38.
- Lu M, Ozelik A, Grigsby CL, et al. (2016). Microfluidic hydrodynamic focusing for synthesis of nanomaterials. *Nano Today* 11:778–92.
- Luo C, Fu Q, Li H, et al. (2005). PDMS microfluidic device for optical detection of protein immunoassay using gold nanoparticles. *Lab Chip* 5:726–9.
- Ma X, Li R, Jin Z, et al. (2020). Injection molding and characterization of PMMA-based microfluidic devices. *Microsyst Technol* 26:1317–24.
- Macdonald NP, Cabot JM, Smejkal P, et al. (2017). Comparing microfluidic performance of three-dimensional (3D) printing platforms. *Anal Chem* 89:3858–66.
- Maeki M, Fujishima Y, Sato Y, et al. (2017). Understanding the formation mechanism of lipid nanoparticles in microfluidic devices with chaotic micromixers. *PLoS One* 12:e0187962.
- Maged A, Mahmoud AA, Salah S, et al. (2020). Spray-dried rosuvastatin nanoparticles for promoting hair growth. *AAPS PharmSciTech* 21:205.
- Mahmoodi Z, Mohammadnejad J, Razavi Bazaz S, et al. (2019). A simple coating method of PDMS microchip with PTFE for synthesis of dexamethasone-encapsulated PLGA nanoparticles. *Drug Deliv Transl Res* 9: 707–20.
- Mahmoodi, L, Bazaz SR, Mohammadnejad J, et al. (2016). Size-tunable alginate nanoparticles synthesis using T-junction microfluidic chip. 2016 23rd Iranian Conference on Biomedical Engineering and 2016 1st International Iranian Conference on Biomedical Engineering (ICBME). IEEE.
- Mahmoudi Z, Mohammadnejad J, Razavi Bazaz S, et al. (2020). Promoted chondrogenesis of hMCSs with controlled release of TGF- β 3 via microfluidics synthesized alginate nanogels. *Carbohydr Polym* 229:115551.
- Manz A, Graber N, Widmer H. (1990). Miniaturized total chemical analysis systems: a novel concept for chemical sensing. *Sens Actuat B* 1: 244–8.
- Marmiroli B, Greci G, Cacho-Nerin F, et al. (2009). Free jet micromixer to study fast chemical reactions by small angle X-ray scattering. *Lab Chip* 9:2063–9.
- Martins JP, Torrieri G, Santos HA. (2018). The importance of microfluidics for the preparation of nanoparticles as advanced drug delivery systems. *Expert Opin Drug Deliv* 15:469–79.
- Masood F. (2016). Polymeric nanoparticles for targeted drug delivery system for cancer therapy. *Mater Sci Eng C Mater Biol Appl* 60:569–78.
- Mata A, Fleischman AJ, Roy S. (2005). Characterization of polydimethylsiloxane (PDMS) properties for biomedical micro/nanosystems. *Biomed Microdevices* 7:281–93.
- Matellan C, Armando E. (2018). Cost-effective rapid prototyping and assembly of poly (methyl methacrylate) microfluidic devices. *Sci Rep* 8:1–13.
- Mathies RA, Huang XC. (1992). Capillary array electrophoresis: an approach to high-speed, high-throughput DNA sequencing. *Nature (Lond)* 359:167–9.
- Melzig S, Finke JH, Schilde C, et al. (2019). Fluid mechanics and process design of high-pressure antisolvent precipitation of fenofibrate nanoparticles using a customized microsystem. *Chem Eng J* 371:554–64.
- Mengeaud V, Josserand J, Girault HH. (2002). Mixing processes in a zig-zag microchannel: finite element simulations and optical study. *Anal Chem* 74:4279–86.
- Minakov A, Rudyak V, Dekterev A, et al. (2013). Investigation of slip boundary conditions in the T-shaped microchannel. *Int J Heat Fluid Flow* 43:161–9.
- Moradikhah F, Doosti-Telgerd M, Shabani I, et al. (2020). Microfluidic fabrication of alendronate-loaded chitosan nanoparticles for enhanced osteogenic differentiation of stem cells. *Life Sci* 254:117768.
- Morikawa Y, Tagami T, Hoshikawa A, et al. (2018). The use of an efficient microfluidic mixing system for generating stabilized polymeric nanoparticles for controlled drug release. *Biol Pharm Bull* 41:899–907.
- Mukherjee P, Nebuloni F, Gao H, et al. (2019). Rapid prototyping of soft lithography masters for microfluidic devices using dry film photoresist in a non-cleanroom setting. *Micromachines* 10:192.
- Niculescu AG, Chircov C, Bircă AC, et al. (2021). Nanomaterials synthesis through microfluidic methods: an updated overview. *Nanomaterials* 11:864.
- Niu G, Ruditskiy A, Vara M, et al. (2015). Toward continuous and scalable production of colloidal nanocrystals by switching from batch to drop-let reactors. *Chem Soc Rev* 44:5806–20.
- Pall Corporation. (2021). Tangential flow filtration. Available at: <https://www.pall.com/en/laboratory/tangential-flow-filtration.html> [cited 11 March 2021].
- Pattni BS, Chupin VV, Torchilin VP. (2015). New developments in liposomal drug delivery. *Chem Rev* 115:10938–66.
- Paxman J, Hunt B, Hallan D, et al. (2017). Drunken membranes: short-chain alcohols alter fusion of liposomes to planar lipid bilayers. *Biophys J* 112:121–32.
- Pessoa AC, Sipoli CC, Lucimara G. (2017). Effects of diffusion and mixing pattern on microfluidic-assisted synthesis of chitosan/ATP nanoparticles. *Lab Chip* 17:2281–93.
- Pol R, Céspedes F, Gabriel D, et al. (2017). Microfluidic lab-on-a-chip platforms for environmental monitoring. *Trac Trends Anal Chem* 95:62–8.
- Raghupathi W, Raghupathi V. (2018). An empirical study of chronic diseases in the United States: a visual analytics approach to public health. *Int J Environ Res Public Health* 15:431.
- Reynolds O. (1883). An experimental investigation of the circumstances which determine whether the motion of water shall be direct or sinuous, and of the law of resistance in parallel channels. *Philos Trans Royal Soc Lond* 1883: 935–82.
- Rhee M, Valencia PM, Rodriguez MI, et al. (2011). Synthesis of size-tunable polymeric nanoparticles enabled by 3D hydrodynamic flow focusing in single-layer microchannels. *Adv Mater* 23:H79–83.
- Riewe J, Erfle P, Melzig S, et al. (2020). Antisolvent precipitation of lipid nanoparticles in microfluidic systems—A comparative study. *Int J Pharm* 579:119167.
- Roces CB, Lou G, Jain N, et al. (2020). Manufacturing considerations for the development of lipid nanoparticles using microfluidics. *Pharmaceutics* 12:1095.
- Romanov V, Samuel R, Chaharlang M, et al. (2018). FDM 3D printing of high-pressure, heat-resistant, transparent microfluidic devices. *Anal Chem* 90:10450–6.
- Ruben B, Elisa M, Leandro L, et al. (2017). Oxygen plasma treatments of polydimethylsiloxane surfaces: effect of the atomic oxygen on capillary flow in the microchannels. *Micro Nano Lett* 12:754–7.
- Sabry MN, El-Emam SH, Mansour MH, et al. (2018). Development of an efficient uniflow comb micromixer for biodiesel production at low Reynolds number. *Chem Eng Proc-Proc Intensificat* 128:162–72.
- Salafi T, Zeming KK, Zhang Y. (2016). Advancements in microfluidics for nanoparticle separation. *Lab Chip* 17:11–33.
- Samae M, Ritmetee P, Chirasatitsin S, et al. (2020). Precise Manufacturing and performance validation of paper-based passive microfluidic micromixers. *Int J Precis Eng Manuf* 21:499–508.
- Santini JT, Cima MJ, Langer R. (1999). A controlled-release microchip. *Nature* 397:335–8.
- Sato Y, Note Y, Maeki M, et al. (2016). Elucidation of the physicochemical properties and potency of siRNA-loaded small-sized lipid nanoparticles for siRNA delivery. *J Control Release* 229:48–57.
- Sato Y, Okabe N, Note Y, et al. (2020). Hydrophobic scaffolds of pH-sensitive cationic lipids contribute to miscibility with phospholipids and improve the efficiency of delivering short interfering RNA by small-sized lipid nanoparticles. *Acta Biomater* 102:341–50.
- Saxena S, Joshi R. (2020). Microfluidic devices: applications and role of surface wettability in its fabrication. *Surface science*. London: IntechOpen.

- Seibt S, Ryan T. (2020). Microfluidics for time-resolved small-angle x-ray scattering. *Advances in micro-and nanofluidics*. London: IntechOpen.
- Serrano P, Decanini D, Leroy L, et al. (2018). Multiflagella artificial bacteria for robust microfluidic propulsion and multimodal micromanipulation. *Microelectron Eng* 195:145–52.
- Shaegh SAM, Pourmand A, Nabavinia M, et al. (2018). Rapid prototyping of whole-thermoplastic microfluidics with built-in microvalves using laser ablation and thermal fusion bonding. *Sens Actuat B* 255:100–9.
- Shanko ES, van de Burgt Y, Anderson PD, et al. (2019). Microfluidic magnetic mixing at low reynolds numbers and in stagnant fluids. *Micromachines (Basel)* 10:731.
- Shembekar N, Chaipan C, Utharala R, et al. (2016). Droplet-based microfluidics in drug discovery, transcriptomics and high-throughput molecular genetics. *Lab Chip* 16:1314–31.
- Shui L, Eijkel JC, van den Berg A. (2007a). Multiphase flow in micro-and nanochannels. *Sens Actuat B* 121:263–76.
- Shui L, Eijkel JC, Van den Berg A. (2007b). Multiphase flow in microfluidic systems -control and applications of droplets and interfaces. *Adv Colloid Interface Sci* 133:35–49.
- Shum HC, Kim JW, Weitz DA. (2008). Microfluidic fabrication of monodisperse biocompatible and biodegradable polymersomes with controlled permeability. *J Am Chem Soc* 130:9543–9.
- Siavashy S, Soltani M, Ghorbani-Bidkobe F, et al. (2021). Microfluidic platform for synthesis and optimization of chitosan-coated magnetic nanoparticles in cisplatin delivery. *Carbohydr Polym* 265:118027.
- Sitanurak J, Fukana N, Wongpakdee T, et al. (2019). T-shirt ink for one-step screen-printing of hydrophobic barriers for 2D-and 3D-microfluidic paper-based analytical devices. *Talanta* 205:120113.
- Sittadjody S, Criswell T, Jackson JD, et al. (2021). Regenerative medicine approaches in bioengineering female reproductive tissues. *Reprod Sci* 28:1573–1595.
- Sivasamy J, Che Z, Neng Wong T, et al. (2010). A simple method for evaluating and predicting chaotic advection in microfluidic slugs. *Chem Eng Sci* 65:5382–91.
- Soheili S, Mandegar E, Moradikhah F, et al. (2021). Experimental and numerical studies on microfluidic preparation and engineering of chitosan nanoparticles. *J Drug Delivery Sci Technol* 61:102268.
- Song H, Ismagilov RF. (2003). Millisecond kinetics on a microfluidic chip using nanoliters of reagents. *J Am Chem Soc* 125:14613–9.
- Stolzenburg P, Lorenz T, Dietzel A, et al. (2018). Microfluidic synthesis of metal oxide nanoparticles via the nonaqueous method. *Chem Eng Sci* 191:500–10.
- Streck S, Clulow AJ, Nielsen HM, et al. (2019a). The distribution of cell-penetrating peptides on polymeric nanoparticles prepared using microfluidics and elucidated with small angle X-ray scattering. *J Colloid Interface Sci* 555:438–48.
- Streck S, Neumann H, Nielsen HM, et al. (2019b). Comparison of bulk and microfluidics methods for the formulation of poly-lactic-co-glycolic acid (PLGA) nanoparticles modified with cell-penetrating peptides of different architectures. *Int J Pharm X* 1:100030.
- Sudarsan AP, Ugaz VM. (2006). Fluid mixing in planar spiral microchannels. *Lab Chip* 6:74–82.
- Sun J, Xianyu Y, Li M, et al. (2013). A microfluidic origami chip for synthesis of functionalized polymeric nanoparticles. *Nanoscale* 5:5262–5.
- Terry SC, Jerman JH, Angell JB. (1979). A gas chromatographic air analyzer fabricated on a silicon wafer. *IEEE Trans Electron Devices* 26:1880–6.
- Therriault D, White SR, Lewis JA. (2003). Chaotic mixing in three-dimensional microvascular networks fabricated by direct-write assembly. *Nat Mater* 2:265–71.
- Thorsen T, Roberts RW, Arnold FH, et al. (2001). Dynamic pattern formation in a vesicle-generating microfluidic device. *Phys Rev Lett* 86:4163–6.
- Tice JD, Song H, Lyon AD, et al. (2003). Formation of droplets and mixing in multiphase microfluidics at low values of the Reynolds and the capillary numbers. *Langmuir* 19:9127–33.
- Utada AS, Lorenceau E, Link DR, et al. (2005). Monodisperse double emulsions generated from a microcapillary device. *Science* 308:537–41.
- Valencia PM, Basto PA, Zhang L, et al. (2010). Single-step assembly of homogenous lipid-polymeric and lipid-quantum dot nanoparticles enabled by microfluidic rapid mixing. *ACS Nano* 4:1671–9.
- Valencia PM, Pridgen EM, Rhee M, et al. (2013). Microfluidic platform for combinatorial synthesis and optimization of targeted nanoparticles for cancer therapy. *ACS Nano* 7:10671–80.
- Van Der Woerd M, Ferree D, Pusey M. (2003). The promise of macromolecular crystallization in microfluidic chips. *J Struct Biol* 142:180–7.
- Vasilescu SA, Bazaz SR, Jin D, et al. (2020). 3D printing enables the rapid prototyping of modular microfluidic devices for particle conjugation. *Appl Mater Today* 20:100726.
- Vasudev A, Kaushik A, Jones K, et al. (2013). Prospects of low temperature co-fired ceramic (LTCC) based microfluidic systems for point-of-care biosensing and environmental sensing. *Microfluid Nanofluid* 14:683–702.
- Vladislavjević GT, Khalid N, Neves MA, et al. (2013). Industrial lab-on-a-chip: design, applications and scale-up for drug discovery and delivery. *Adv Drug Deliv Rev* 65:1626–63.
- Vu HTH, Streck S, Hook SM, et al. (2019). Utilization of microfluidics for the preparation of polymeric nanoparticles for the antioxidant rutin: a comparison with bulk production. *Pharm Nanotechnol* 7:469–83.
- Wagner J, Köhler J. (2005). Continuous synthesis of gold nanoparticles in a microreactor. *Nano Lett* 5:685–91.
- Wang H, Chen B, He M, et al. (2019). Study on uptake of gold nanoparticles by single cells using droplet microfluidic chip-inductively coupled plasma mass spectrometry. *Talanta* 200:398–407.
- Wang CT, Hu YC, Hu TY. (2009). Biophysical micromixer. *Sensors (Basel)* 9:5379–89.
- Webb C, Forbes N, Roces CB, et al. (2020). Using microfluidics for scalable manufacturing of nanomedicines from bench to GMP: a case study using protein-loaded liposomes. *Int J Pharm* 582:119266.
- Woolley AT, Mathies RA. (1994). Ultra-high-speed DNA fragment separations using microfabricated capillary array electrophoresis chips. *Proc Natl Acad Sci USA* 91:11348–52.
- Xu J, Zhang S, Machado A, et al. (2017). Controllable microfluidic production of drug-loaded PLGA nanoparticles using partially water-miscible mixed solvent microdroplets as a precursor. *Sci Rep* 7:1–12.
- Yang Z, Goto H, Matsumoto M, et al. (2000). Active micromixer for microfluidic systems using lead-zirconate-titanate (PZT)-generated ultrasonic vibration. *Electrophoresis* 21:116–9.
- Yang Z, Matsumoto S, Goto H, et al. (2001). Ultrasonic micromixer for microfluidic systems. *Sens Actuat A* 93:266–72.
- Yaralioglu GG, Wygant IO, Marentis TC, et al. (2004). Ultrasonic mixing in microfluidic channels using integrated transducers. *Anal Chem* 76:3694–8.
- Yen BKH, Günther A, Schmidt MA, et al. (2005). A microfabricated gas-liquid segmented flow reactor for high-temperature synthesis: the case of CdSe quantum dots. *Angew Chem Int Ed Engl* 44:5447–51.
- Yeung C, Chen S, King B, et al. (2019). A 3D-printed microfluidic-enabled hollow microneedle architecture for transdermal drug delivery. *Biomicrofluidics* 13:064125.
- Younis MA, Khalil IA, Elewa YHA, et al. (2021). Ultra-small lipid nanoparticles encapsulating sorafenib and midkine-siRNA selectively-eradicate sorafenib-resistant hepatocellular carcinoma in vivo. *J Control Release* 331:335–49.
- Yu Z, Hemminger O, Fan LS. (2007). Experiment and lattice Boltzmann simulation of two-phase gas-liquid flows in microchannels. *Chem Eng Sci* 62:7172–83.
- Zhang L, Chen Q, Ma Y, et al. (2020). Microfluidic methods for fabrication and engineering of nanoparticle drug delivery systems. *ACS Appl Bio Mater* 3:107–20.
- Zhang Y, Yesiloz G, Sharahi HJ, et al. (2019). Geomaterial-functionalized microfluidic devices using a universal surface modification approach. *Adv Mater Interfaces* 6:1900995.

- Zhao CX, He L, Qiao SZ, et al. (2011). Nanoparticle synthesis in microreactors. *Chem Eng Sci* 66:1463–79.
- Zheng F, Xiao Y, Liu H, et al. (2021). Patient-specific organoid and organ-on-a-chip: 3D cell-culture meets 3D printing and numerical simulation. *Adv Biol (Weinh)* 5:e2000024.
- Zhigaltsev IV, Belliveau N, Hafez I, et al. (2012). Bottom-up design and synthesis of limit size lipid nanoparticle systems with aqueous and triglyceride cores using millisecond microfluidic mixing. *Langmuir* 28:3633–40.
- Zhu J, Wang M, Zhang H, et al. (2020). Effects of hydrophilicity, adhesion work, and fluid flow on biofilm formation of PDMS in microfluidic systems. *ACS Appl Bio Mater* 3:8386–94.